

ADAPTABLE HIGH-DIMENSIONAL CHANGE POINT DETECTION VIA RIDGE REGULARIZATION

BY HAORAN LI^{*1,a} AND HAOTIAN XU^{1,b}

¹Department of Mathematics and Statistics, Auburn University, ^ahzl0152@auburn.edu; ^bhaotian.xu@auburn.edu

We study the problem of detecting multiple change points in the mean vectors of an independent sequence of high-dimensional observations. We propose a family of ridge-regularized CUSUM statistics built upon the adaptable ridge-regularized Hotelling's T^2 test of Li et al. (Ann. Statist. **48** (2020) 1815–1847). The proposed tests are designed for dense alternatives in the high-dimensional regime where the dimension is comparable to the sample size. By introducing ridge regularization, the procedure achieves a stable form of sample covariance normalization and attains adaptability with respect to the underlying population covariance structure. We derive the limiting distributions of the proposed statistics under mild conditions, both under the null hypothesis and under a class of local alternatives. We further develop a principled framework for selecting the regularization parameter by maximizing asymptotic power. Extensive simulation studies demonstrate that the proposed tests compare favorably with a wide range of existing methods across diverse settings. The performance of the proposed test procedure is illustrated through an application to a panel of daily log-returns from S&P 500 constituents spanning 2007–2025.

1. Introduction. Change point detection is a classical problem in statistics with applications across a wide range of disciplines, including econometrics, signal processing, and climate science. In this setting, one observes an ordered sequence of random vectors $X_1, X_2, \dots, X_n \in \mathbb{R}^p$ that are independent and identically distributed, except for possible structural changes in their mean vectors. In this paper, we consider the model

$$(1.1) \quad X_j = \mu_j + \Sigma_p^{1/2} Z_j, \quad j = 1, \dots, n,$$

where $\{\mu_j\}$ is a sequence of mean vectors, $\{Z_j\} \in \mathbb{R}^p$ are i.i.d. random vectors with independent, mean-zero, unit-variance entries, and Σ_p is a general covariance matrix. Under the null hypothesis of no change point, the mean vectors are constant over time, that is,

$$H_0 : \mu_j \equiv \mu, \quad j = 1, \dots, n.$$

We are interested in testing H_0 against the alternative that the mean vector undergoes a finite number of abrupt changes:

$$(1.2) \quad H_a : \mu_1 = \dots = \mu_{k_1} \neq \mu_{k_1+1} = \dots = \mu_{k_s} \neq \mu_{k_s+1} = \dots = \mu_n,$$

where $s \geq 1$ and $\{k_j\}_{j=1}^s \in [1, n)$ denote the (unknown) number and locations of change points. We henceforth refer to H_a as the multiple change point (MC) alternative.

In the classical regime where the dimension p is fixed and small, change point detection has been extensively studied; see Csörgő and Horváth (1997) and Aue and Horváth (2013) for comprehensive reviews of classical methods. To motivate the ideas, consider the case $s = 1$. That is, we are interested in testing H_0 against the alternative

$$H_a^{\text{SC}} : \mu_1 = \dots = \mu_{k_1} \neq \mu_{k_1+1} = \dots = \mu_n,$$

*Corresponding author.

MSC2020 subject classifications: Primary 62H15, 62J05; secondary 60B20.

Keywords and phrases: Ridge regularization, Random Matrix Theory.

which we henceforth refer to as the single change-point (SC) alternative. For simplicity, assume that the covariance matrix Σ_p is non-singular and known. The classical CUSUM approach compares the sample means of the two segments $\{X_1, \dots, X_k\}$ and $\{X_{k+1}, \dots, X_n\}$, normalized by $\Sigma_p^{-1/2}$, over all possible change point locations k . Specifically, the CUSUM test statistic takes the form

$$\max_{1 \leq k \leq n-1} C_0(k)^T \Sigma_p^{-1} C_0(k),$$

where $C_0(k) = \frac{1}{n-k} \sum_{j=k+1}^n X_j - \frac{1}{k} \sum_{j=1}^k X_j$ denotes the difference between the sample means of the two segments separated at k . In the low-dimensional regime and under the null hypothesis H_0 , Σ_p can be consistently estimated by the pooled sample covariance matrix

$$(1.3) \quad S_n = \frac{1}{n} \sum_{j=1}^n (X_j - \bar{X})(X_j - \bar{X})^T, \quad \text{with } \bar{X} = \frac{1}{n} \sum_{j=1}^n X_j.$$

The CUSUM procedure can therefore be implemented by replacing Σ_p with S_n . Importantly, under H_0 , the distribution of the resulting test statistic, whether normalized by Σ_p^{-1} or by S_n^{-1} , is invariant with respect to Σ_p , which highlights the robustness of classical methods to the unknown covariance structure.

High-dimensional data are now ubiquitous in many scientific fields. When the dimension p is comparable to or larger than the sample size n , the performance of traditional methods deteriorates substantially. First, accurate estimation of the precision matrix Σ_p^{-1} becomes challenging in this regime, particularly in the absence of structural assumptions, such as low-rank structure or sparsity. Second, the accumulation of noise across coordinates fundamentally alters the limiting distributions of classical test statistics.

There is a substantial literature on change point testing and estimation for the mean of high-dimensional data. Broadly speaking, existing methods can be classified into three main categories. The first class focuses on detecting sparse mean changes, where only a small subset of components of the mean vector undergo change over time. These methods typically rely on the ℓ_∞ -norm of the mean difference $C_0(k)$ and include, among others, [Jiřák \(2015\)](#) and [Yu and Chen \(2021\)](#). The second class targets dense alternatives, in which the signal may be distributed across many or all coordinates. For example, [Zhang et al. \(2010\)](#) and [Zhang and Lavitas \(2018\)](#) consider tests based on the ℓ_2 -norm of $C_0(k)$ without normalization by Σ_p^{-1} , while [Wang et al. \(2022\)](#) proposes a modified procedure motivated by U-statistic techniques. The third class comprises methods that do not presuppose specific alternative structures, such as projection-based approaches [Wang and Samworth \(2018\)](#) and [Enikeeva and Harchaoui \(2019\)](#). Other notable works include [Shao and Zhang \(2010\)](#); [Matteson and James \(2014\)](#); [Kirch et al. \(2015\)](#); [Cho \(2016\)](#); [Liu et al. \(2020\)](#); [Zhang et al. \(2022\)](#).

While most existing methods largely overlook the role of covariance scaling and directly utilize the norm of $C_0(k)$, we propose a new class of test statistics that achieve data-driven covariance normalization by scaling the observations with a ridge-regularized sample covariance estimator. Specifically, we transform the observations according to

$$(S_n + \lambda I_p)^{-1/2} X_j, \quad j = 1, \dots, n,$$

where S_n denotes the pooled sample covariance matrix and $\lambda > 0$ is a tuning parameter. Targeting dense alternatives, we construct test statistics based on the ℓ_2 -norm of the resulting scaled observations; see (2.3). Our methodology builds on the ridge-regularized Hotelling's T^2 (RHT) test for comparing two high-dimensional mean vectors, as proposed in [Chen et al. \(2011\)](#) and further developed in [Li et al. \(2020b\)](#).

Importantly, the resulting test statistics are *rotation-invariant*, in the sense that their values are unchanged under arbitrary orthogonal transformations of the data, that is, when X_j is

replaced by $Q^T X_j$ for any orthogonal matrix Q^T . This invariance is a desirable property when not much prior knowledge about Σ_p and the alternative is available.

We work in a high-dimensional regime where the dimension p is comparable to the sample size n , in the sense that $p/n \rightarrow \gamma \in (0, \infty)$. Detecting dense alternatives in this regime is well motivated by a variety of applications. For example, KEGG pathway-level analyses of DNA copy number alteration (CNA) patterns often involve a few hundred genes, and substantial empirical evidence suggests that such alterations in a cancer cell occur across a large fraction of genes rather than being confined to a few isolated components (Graham et al., 2017). In climate science, spatio-temporal fields are often represented using tens to a few hundred spatial locations or principal components, and regime changes typically induce coherent mean shifts across a large fraction of these components (DeFriez et al., 2016). In neuroimaging, brain activity is frequently summarized over a few hundred regions of interest, and transitions between cognitive or behavioral states are associated with widespread changes across many regions, resulting in dense mean shifts in moderately high-dimensional signals (Kringelbach and Deco, 2020).

Technically, in the regime $p/n \rightarrow \gamma$, fundamental results from *Random Matrix Theory* (RMT) indicate that, although the pooled sample covariance matrix S_n is a biased estimator of Σ_p under H_0 , it exhibits stable limiting spectral behavior under mild conditions, determined solely by the spectral distribution of Σ_p and the limiting ratio γ . The introduction of a ridge term λI_p shifts the spectrum of S_n away from singularity while preserving its essential spectral structure. As a consequence, the ridge-regularized matrix $(S_n + \lambda I_p)^{-1}$ retains meaningful structural information about the underlying precision matrix Σ_p^{-1} . The resulting ℓ_2 -norm-based procedures are therefore expected to achieve robustness with respect to the unknown covariance structure.

Our work focuses on the case where the number of change points s is unknown and arbitrary, while the simpler case $s = 1$ is discussed explicitly for the reader's convenience. Moreover, we assume that the change-point locations k_j are bounded away from the endpoints (1 and n) of the observation sequence and scale proportionally with the sample size, in the sense that $k_j/n \rightarrow \tilde{t}_j \in (0, 1)$ for all $j = 1, \dots, s$. When s is unknown, we adopt flexible scanning techniques in which differences between sample means are compared across multi-scale adjacent segments of the observations.

The rest of the paper is organized as follows. In Section 2, we present the proposed test statistics for both the single and multiple change-point scenarios when λ is given. In Section 3, after introducing the necessary preliminaries from RMT, we derive the asymptotic null distributions of the proposed test statistics. These limiting distributions are shown to be pivotal; consequently, the critical values of the proposed tests can be tabulated or computed numerically, making the procedures easy to implement. We also study the asymptotic power of the tests under two frameworks: a class of deterministic local alternatives and a class of probabilistic local alternatives, in which the mean shifts are treated as realizations from prior distributions. The problem of selecting the regularization parameter λ is discussed in Section 4. A simulation study is reported in Section 5, where we compare the proposed methods with several existing methods in the literature under various representative settings. A real data application to daily log-returns from constituents of the S&P 500 index spanning 2007–2025 is presented in Section 6. Finally, in Section 7, we discuss the proposed methods and possible extensions, particularly to time series settings. Technical details and additional simulation results are provided in the Supplementary Material.

2. Method. In this section, we present the proposed methodology for a given regularization parameter $\lambda > 0$. For $t \in (0, 1)$, we define

$$k(t) = \lfloor nt \rfloor + 1.$$

We say that an observation X_j , $j = 1, \dots, n$ belongs to the segment $[t_1, t_2)$ if $k(t_1) \leq j < k(t_2)$. The average of all observations belonging to a given segment is referred to as the corresponding segment mean.

Denote the set of all ordered triples in $[0, 1]$ by

$$\mathcal{A} = \{(t_1, t_2, t_3) \in [0, 1]^3 : t_1 < t_2 < t_3\}.$$

Then, any element of \mathcal{A} defines two adjacent segments $[t_1, t_2)$ and $[t_2, t_3)$. We consider the difference between the corresponding sample segment means normalized by $(S_n + \lambda I_p)^{-1/2}$, where S_n denotes the pooled sample covariance matrix defined in (1.3). Specifically, denote

$$(2.1) \quad C_\lambda(t_1, t_2, t_3) = (S_n + \lambda I_p)^{-1/2} \left(\frac{1}{k(t_3) - k(t_2)} \sum_{j=k(t_2)}^{k(t_3)-1} X_j - \frac{1}{k(t_2) - k(t_1)} \sum_{j=k(t_1)}^{k(t_2)-1} X_j \right).$$

Here, we assume that each segment contains at least one observation. We further define the associated effective sample size by

$$(2.2) \quad N(t_1, t_2, t_3) = \frac{(k(t_2) - k(t_1))(k(t_3) - k(t_2))}{k(t_3) - k(t_1)}.$$

We define the ridge-regularized statistic as

$$(2.3) \quad V_\lambda(t_1, t_2, t_3) = N(t_1, t_2, t_3) \|C_\lambda(t_1, t_2, t_3)\|_2^2$$

where $\|\cdot\|_2$ is the Euclidean norm of a vector or the spectral norm of a matrix. The theoretical analysis in Section 3 shows that the asymptotic mean and variance of $V_\lambda(t_1, t_2, t_3)$ depend on the underlying covariance matrix Σ_p . To eliminate this dependence and standardize the statistic, we introduce

$$(2.4) \quad \begin{aligned} \hat{\Theta}(\lambda) &= [1 - \lambda m_n(-\lambda)], \\ \hat{\Gamma}(\lambda) &= 2[1 - \gamma_n + \gamma_n \lambda m_n(-\lambda)][1 - \lambda m_n(-\lambda)] - 2[\lambda m_n(-\lambda) - \lambda^2 m'_n(-\lambda)], \end{aligned}$$

where $\gamma_n = p/(n-1)$ and

$$(2.5) \quad m_n(-\lambda) = \frac{1}{p} \text{tr} \left[\left(\frac{n}{n-1} S_n + \lambda I_p \right)^{-1} \right], \quad m'_n(-\lambda) = \frac{1}{p} \text{tr} \left[\left(\frac{n}{n-1} S_n + \lambda I_p \right)^{-2} \right].$$

We then define the standardized statistic

$$(2.6) \quad D_\lambda(t_1, t_2, t_3) = \sqrt{p} \frac{p^{-1} V_\lambda(t_1, t_2, t_3) - \hat{\Theta}(\lambda)}{\sqrt{\hat{\Gamma}(\lambda)}}.$$

In Section 3, we show that $D_\lambda(t_1, t_2, t_3)$ has asymptotic mean zero and unit variance under mild regularity conditions. Note that both $\hat{\Theta}(\lambda)$ and $\hat{\Gamma}(\lambda)$ depend only on the eigenvalues of S_n and the aspect ratio γ_n .

While the proposed statistic $V_\lambda(t_1, t_2, t_3)$ is motivated by the ridge-regularized Hotelling's T^2 (RHT) statistic proposed in Li et al. (2020b) for the two-sample mean testing problem, the statistic $V_\lambda(t_1, t_2, t_3)$ differs from the RHT statistic in the choice of the scaling matrix. The latter uses a ridge-regularized sample covariance matrix in which each observation X_j is centered by the corresponding segment mean rather than by the overall mean \bar{X} , as in S_n . This difference in centering and scaling leads to different asymptotic means and variances.

The different choices of scaling matrices originate from the fundamentally different problem settings of change-point detection and two-sample mean testing. The scaling matrix used in the RHT statistic has the advantage of being unbiased under both H_0 and H_a in the two-sample mean testing problem, where the group membership is known. However, in

the change-point detection setting, especially when more than one change-point may exist, the locations of potential break points are unknown and the test must scan over a collection of triples (t_1, t_2, t_3) . In this case, the scaling matrix used in RHT generally becomes biased under the alternative and, moreover, depends on the specific triple. When scanning over a large collection of triples, repeatedly evaluating and inverting this scaling matrix incurs a substantial computational burden.

Single change point. As a simple yet informative special case, we first focus on the single change point alternative. Throughout the analysis, we assume that a user-specified trimming parameter $\varepsilon \in (0, 0.5)$ is fixed. In our implementation, we select $\varepsilon = 0.1$. We propose a test based on the statistic

$$(2.7) \quad T_{\text{sc}}(\varepsilon, \lambda) = \max_{t \in [\varepsilon, 1-\varepsilon]} D_\lambda(0, t, 1).$$

This statistic scans over all binary partitions of the interval $[0, 1]$ such that each segment has length at least ε . For each candidate partition, the difference between the two segment means is quantified by the standardized statistic $D_\lambda(0, t, 1)$.

Multiple change points. When multiple change points are present under the alternative, the scanning strategy as in (2.7) may suffer from power loss, as one of the two segments $[0, t]$ or $[t, 1]$ will contain multiple change points. In such cases, opposing mean shifts may cancel each other, leading to little or no change in the segment means. This issue is particularly pronounced when the mean shifts exhibit a nonmonotonic pattern. It is therefore desirable to develop a test that is adaptive, in the sense that it maintains reasonable power without requiring prior knowledge of the number of change points s under the alternative.

Motivated by this consideration, we propose to scan over multi-scale adjacent segments whose lengths are at least ε . To this end, we define the scanning set

$$(2.8) \quad \mathcal{T}(\varepsilon) = \{(t_1, t_2, t_3) \in [0, 1]^3 : t_2 - t_1 \geq \varepsilon, t_3 - t_2 \geq \varepsilon\}$$

We propose to test H_0 against the MC alternative H_a by the statistic

$$T_{\text{mc}}(\varepsilon, \lambda) = \max_{(t_1, t_2, t_3) \in \mathcal{T}(\varepsilon)} D_\lambda(t_1, t_2, t_3).$$

From a practical point of view, the computation of D_λ at any given triple (t_1, t_2, t_3) is fast and efficient, provided that the eigendecomposition of S_n is available. Indeed, using the eigenvectors and eigenvalues of S_n , we first transform the observations according to $(S_n + \lambda I_p)^{-1/2} X_j$, $j = 1, \dots, n$. Given the transformed data, the computational complexity of evaluating $D_\lambda(t_1, t_2, t_3)$ is $O(pn)$. However, the computation of $T_{\text{mc}}(\varepsilon, \lambda)$ requires evaluating $D_\lambda(t_1, t_2, t_3)$ over $O(n^3)$ candidate triples, which can incur a substantial computational burden when both n and p are large.

To alleviate this burden, we consider a discretized version of the scanning set, defined as

$$(2.9) \quad \mathcal{T}_*(\varepsilon) = \mathcal{T}(\varepsilon) \cap \{\mathcal{G}(\varepsilon)\}^3, \quad \mathcal{G}(\varepsilon) = \{j\varepsilon : j \in \mathbb{Z}\}.$$

That is, we restrict t_j 's to be a multiple of ε . The resulting computationally efficient test statistic is given by

$$T_{\text{mc}}^*(\varepsilon, \lambda) = \max_{(t_1, t_2, t_3) \in \mathcal{T}_*(\varepsilon)} D_\lambda(t_1, t_2, t_3).$$

Given the transformed data, the computational complexity of computing $T_{\text{mc}}^*(\varepsilon)$ is $O(pn\varepsilon^{-3})$, which remains manageable even when both p and n are large. Similar discretization strategies have been adopted in the literature; see, for example, [Zhang and Lavitas \(2018\)](#)

and Wang et al. (2022). Compared with these existing approaches, our scanning strategy is more flexible. In particular, in Zhang and Lavitas (2018) and Wang et al. (2022), either t_1 is fixed at 0 or t_3 is fixed at 1, whereas in our method all three time points are allowed to vary. As a result, we scan over a richer collection of multi-scale segments, which is expected to improve the ability of the proposed method to capture abrupt changes occurring in the central part of the observation period.

3. Asymptotic Theory. After giving the necessary preliminaries on RMT, the asymptotic theory of the proposed tests under the null hypothesis and under various local alternative models is presented in this section.

3.1. *Settings.* We make the following assumptions on the model. Let $\tau_{1,p} \geq \dots \geq \tau_{p,p} \geq 0$ denote the eigenvalues of Σ_p , and define

$$H_p(\tau) = \frac{1}{p} \sum_{j=1}^p \mathbb{1}_{[\tau_{j,p}, \infty)}(\tau)$$

to be the spectral distribution function of Σ_p . We henceforth refer to H_p as the *population spectral distribution function* (PSD).

- C1** *Moment conditions.* The entries of $\{Z_j\}$ have finite fourth moments.
- C2** *High-dimensional regime.* As $p, n \rightarrow \infty$, we assume that $\gamma_n = p/(n-1) \rightarrow \gamma \in (0, \infty)$.
- C3** *Location of breaks.* We assume that s is fixed. If $s > 0$, the locations k_s is such that for some $\tilde{t}_1 < \tilde{t}_2 < \dots < \tilde{t}_s \in (0, 1)$, $k_j/n \rightarrow \tilde{t}_j$, $j = 1, \dots, s$, as $p, n \rightarrow \infty$.
- C4** *Boundedness of the spectral norm.* The covariance matrix Σ_p is nonnegative definite and satisfies $\limsup_{p \rightarrow \infty} \tau_{1,p} < \infty$.
- C5** *Asymptotic stability of the PSD.* The PSD H_p converges weakly to a probability distribution function H as $p \rightarrow \infty$, where H is not the Dirac measure at 0. We henceforth refer to H as the limiting PSD.

The above conditions are mild. First, we establish the asymptotic behavior of the proposed statistic under low-order moment assumptions, as specified in **C1**. Second, **C2** places the problem in a high-dimensional regime in which the dimension p and the sample size n grow proportionally. This setting has been extensively studied in RMT, and the asymptotic eigenvalue behavior of S_n is well understood under this regime. Third, **C3** requires the locations of the change points to be bounded away from 0 and 1, which is a standard assumption in the high-dimensional change point detection literature. Fourth, **C4** imposes a uniform bound on the eigenvalues of Σ_p . Finally, **C5** ensures that the population spectral distribution stabilizes to a non-degenerate limit.

3.2. *Preliminaries on Random Matrix Theory.* In this section, we present fundamental results from RMT concerning the asymptotic behavior of the spectral distribution of S_n under the null hypothesis H_0 . The results summarized here can be found, for example, in Bai and Silverstein (2004); Li et al. (2020a); Paul and Aue (2014); Knowles and Yin (2017).

Denote the eigenvalues of the sample covariance matrix S_n to be $\alpha_1 \geq \dots \geq \alpha_p$. We consider the spectral distribution function of S_n , defined as

$$F_p(\tau) = \frac{1}{p} \sum_{j=1}^p \mathbb{1}_{[\alpha_j, \infty)}(\tau).$$

We henceforth refer to F_p as the *empirical spectral distribution* (ESD).

Recall that the Stieltjes transform $\varphi_G(\cdot)$ of any function G of bounded variation on \mathbb{R} is defined by

$$\varphi_G(z) = \int_{-\infty}^{\infty} \frac{dG(\tau)}{\tau - z}, \quad z \in \mathbb{C}^+ := \{u + iv : v > 0\}.$$

Consider any compactly supported distribution function F , excluding the Dirac measure at 0. Then, for any $c > 0$, the famous Marčenko-Pastur (M-P) equation in RMT is defined for any $z \in \mathbb{C}^+$ as

$$(3.1) \quad \varphi = \int \frac{dF(\tau)}{\tau(1 - c - cz\varphi) - z}.$$

It is well known that there exists a unique solution $\varphi = \varphi(z; c, F) \in \mathbb{C}^+$ to (3.1). The function $\varphi(z)$ is the Stieltjes transform of a probability measure with bounded support in $[0, \infty)$. Unfortunately, except in extreme cases where F has a simple structure, there is no explicit closed-form for $\varphi(z)$ or the associated probability measure. Moreover, the function $\varphi(z) = \varphi(z; c, F)$ is analytic on \mathbb{C}^+ and admits a smooth extension to the negative real axis \mathbb{R}_- . With a slight abuse of notation, we continue to denote this extension as

$$\varphi(x; c, F) := \lim_{z \in \mathbb{C}^+ \rightarrow x} \varphi(z; c, F), \quad \text{for } x \in \mathbb{R}_-.$$

The subsequent analysis will primarily focus on this domain. For further details of M-P equation, see Chapter 3 of [Bai and Silverstein \(2010\)](#) and [Paul and Aue \(2014\)](#).

We are particularly interested in the M-P equation evaluated as $F = H_p$ and $c = \gamma_n$. We shall write $\varphi_n(x) = \varphi(x; \gamma_n, H_p)$, $x \in \mathbb{R}_-$, in the subsequent analysis. The asymptotic behavior of the sample covariance matrix S_n under the null hypothesis H_0 is closely related to $\varphi_n(x)$ in the following sense.

For $\lambda > 0$, define the deterministic counterpart of $\hat{\Theta}(\lambda)$ and $\hat{\Gamma}(\lambda)$ as

$$(3.2) \quad \begin{aligned} \Theta_n(\lambda) &= 1 - \lambda\varphi_n(-\lambda), \\ \Gamma_n(\lambda) &= 2[1 - \gamma_n + \gamma_n\lambda\varphi_n(-\lambda)][1 - \lambda\varphi_n(-\lambda)] - 2[\lambda\varphi_n(-\lambda) - \lambda^2\varphi_n'(-\lambda)]. \end{aligned}$$

Further, define the *deterministic equivalent* matrix

$$(3.3) \quad \mathcal{D}_n(\lambda) = \left[(1 - \gamma_n + \gamma_n\lambda\varphi_n(-\lambda))\Sigma_p + \lambda I_p \right]^{-1}.$$

LEMMA 3.1. *Suppose that H_0 holds. Under Conditions **C1–C5**, consider any compact interval $[\underline{\lambda}, \bar{\lambda}]$ with $\bar{\lambda} > \underline{\lambda} > 0$. The following statements hold.*

(i) *We have*

$$\sup_{\lambda \in [\underline{\lambda}, \bar{\lambda}]} \sqrt{n} |m_n(-\lambda) - \varphi_n(-\lambda)| \xrightarrow{P} 0, \quad \sup_{\lambda \in [\underline{\lambda}, \bar{\lambda}]} \sqrt{n} |m_n'(-\lambda) - \varphi_n'(-\lambda)| \xrightarrow{P} 0.$$

(ii) *Consequently,*

$$\sup_{\lambda \in [\underline{\lambda}, \bar{\lambda}]} \sqrt{n} |\hat{\Theta}(\lambda) - \Theta_n(\lambda)| \xrightarrow{P} 0, \quad \sup_{\lambda \in [\underline{\lambda}, \bar{\lambda}]} \sqrt{n} |\hat{\Gamma}(\lambda) - \Gamma_n(\lambda)| \xrightarrow{P} 0.$$

Further, we can find a constant $\mathcal{K} > 0$ such that $\inf_{\lambda \in [\underline{\lambda}, \bar{\lambda}]} |\Gamma_n(\lambda)| > \mathcal{K}$ for all sufficiently large n . The constant \mathcal{K} depends only on $\underline{\lambda}$ and $\bar{\lambda}$.

(iii) *For any sequence of symmetric matrices A with uniformly bounded operator norm,*

$$\sup_{\lambda \in [\underline{\lambda}, \bar{\lambda}]} \sqrt{n} |p^{-1} \text{tr}[(S_n + \lambda I_p)^{-1} A] - p^{-1} \text{tr}[\mathcal{D}_n(\lambda) A]| \xrightarrow{P} 0.$$

Lemma 3.1 can be extended to the alternative hypothesis H_a . See Section 3.4.1 for details.

The result in (iii) of Lemma 3.1 is particularly insightful for the proposed method. It demonstrates that $\mathcal{D}_n(\lambda)$ can be viewed as the *deterministic equivalent* of the ridge-regularized inverse $(S_n + \lambda I_p)^{-1}$, when $p/n \rightarrow \gamma$. Importantly, $\mathcal{D}_p(\lambda)$ shares the same eigenvectors as Σ_p^{-1} , while its eigenvalues are transformed through a nonlinear mapping induced by the ridge regularization. This mapping preserves the ordering of the eigenvalues. In this sense, $(S_n + \lambda I_p)^{-1}$ preserves the essential spectral structure of the underlying precision matrix Σ_p^{-1} .

3.3. Asymptotic Null Distribution. In this section, we derive the asymptotic distribution of the proposed statistics under the null hypothesis H_0 . Throughout the analysis, we fix the regularization parameter λ and the trimming parameter ε .

We introduce the following auxiliary functions. For an ordered triple $(t_1, t_2, t_3) \in \mathcal{A}$, define

$$(3.4) \quad u(x; t_1, t_2, t_3) = \begin{cases} 0, & 0 \leq x < t_1, \\ -1/(t_2 - t_1), & t_1 \leq x < t_2, \\ 1/(t_3 - t_2), & t_2 \leq x < t_3, \\ 0, & t_3 \leq x \leq 1. \end{cases}$$

Denote the inner product between $u(\cdot; t_1, t_2, t_3)$ and $u(\cdot; m_1, m_2, m_3)$ by

$$(3.5) \quad \kappa(t_1, t_2, t_3; m_1, m_2, m_3) = \int_0^1 u(x; t_1, t_2, t_3) u(x; m_1, m_2, m_3) dx.$$

We shall write the squared norm $\kappa(t_1, t_2, t_3; t_1, t_2, t_3)$ simply as $\kappa(t_1, t_2, t_3)$.

We introduce a centered Gaussian process $\{G(t_1, t_2, t_3), (t_1, t_2, t_3) \in \mathcal{A}\}$ with covariance kernel

$$\mathbb{E}G(t_1, t_2, t_3)G(m_1, m_2, m_3) = \frac{(\kappa(t_1, t_2, t_3; m_1, m_2, m_3))^2}{\kappa(t_1, t_2, t_3)\kappa(m_1, m_2, m_3)},$$

for $(t_1, t_2, t_3), (m_1, m_2, m_3) \in \mathcal{A}$. It is straightforward that the kernel is nonnegative definite and the increment variance $\mathbb{E}(G(t_1, t_2, t_3) - G(m_1, m_2, m_3))^2$ is Hölder continuous in (t_1, t_2, t_3) and (m_1, m_2, m_3) . By Kolmogorov's continuity theorem, the process is well defined and admits a modification with almost surely continuous sample paths. Finally, $G(t_1, t_2, t_3)$ is pivotal and its distribution can be simulated.

THEOREM 3.1 (Single Change Point). *Suppose that Conditions C1–C5 hold. Under the null hypothesis H_0 , for any fixed $\lambda > 0$ and $\varepsilon > 0$, we have*

$$T_{\text{sc}}(\varepsilon, \lambda) \xrightarrow{D} \sup_{t \in [\varepsilon, 1-\varepsilon]} G(0, t, 1).$$

In practice, given $\lambda > 0$, $\varepsilon \in (0, 0.5)$, and $\alpha \in (0, 1)$, we reject the null hypothesis H_0 in favor of the single change point alternative H_a^{SC} at the asymptotic significance level α , if

$$T_{\text{sc}}(\varepsilon, \lambda) > \xi_{\text{sc}}(1 - \alpha, \varepsilon),$$

where $\xi_{\text{sc}}(1 - \alpha, \varepsilon)$ is the $(1 - \alpha)$ -quantile of the distribution of $\sup_{t \in [\varepsilon, 1-\varepsilon]} G(0, t, 1)$. In Appendix A, we present a table of simulated quantiles for representative choices of α and ε .

THEOREM 3.2 (Multiple Change Points). *Suppose that Conditions C1–C5 hold. Under the null hypothesis H_0 , for any fixed $\lambda > 0$ and $\varepsilon > 0$, we have*

$$T_{\text{mc}}(\varepsilon, \lambda) \xrightarrow{D} \sup_{(t_1, t_2, t_3) \in \mathcal{T}(\varepsilon)} G(t_1, t_2, t_3);$$

$$T_{\text{mc}}^*(\varepsilon, \lambda) \xrightarrow{D} \sup_{(t_1, t_2, t_3) \in \mathcal{T}_*(\varepsilon)} G(t_1, t_2, t_3).$$

In practice, given $\lambda > 0$, $\varepsilon \in (0, 0.5)$, and $\alpha \in (0, 1)$, we reject the null hypothesis H_0 in favor of the general alternative H_a at the asymptotic significance level α , if

$$T_{\text{mc}}(\varepsilon, \lambda) > \xi_{\text{mc}}(1 - \alpha, \varepsilon),$$

where $\xi_{\text{mc}}(1 - \alpha, \varepsilon)$ is the $(1 - \alpha)$ -quantile of the distribution of $\sup_{\mathcal{T}(\varepsilon)} G(t_1, t_2, t_3)$.

Alternatively, we may adopt the computationally efficient test

$$T_{\text{mc}}^*(\varepsilon, \lambda) > \xi_{\text{mc}}^*(1 - \alpha, \varepsilon),$$

where $\xi_{\text{mc}}^*(1 - \alpha, \varepsilon)$ is the $(1 - \alpha)$ -quantile of the distribution of $\sup_{\mathcal{T}_*(\varepsilon)} G(t_1, t_2, t_3)$. In Appendix A, we present a table of simulated quantiles for representative choices of α and ε .

3.4. Asymptotic Distribution Under Local Alternatives. In this section, we study the behavior of the proposed test under two types of local alternatives: deterministic local alternatives and probabilistic local alternatives. The analysis is carried out both for the insightful special case of a single change point and for the general multiple change-point setting. Throughout, we consider a fixed trimming parameter ε and the significance level α .

3.4.1. Shift of the sample covariance matrix under H_a . We define the oracle sample covariance matrix constructed from the correctly centered observations by

$$\tilde{S}_n = \frac{1}{n} \sum_{j=1}^n \Sigma_p^{1/2} (Z_j - \bar{Z}) (Z_j - \bar{Z})^T \Sigma_p^{1/2},$$

where $\bar{Z} = n^{-1} \sum_{j=1}^n Z_j$. Let $\Delta_n = S_n - \tilde{S}_n$. Then, it is immediate that $\Delta_n = 0$ under H_0 . Thus, Δ_n represents the shift of S_n under H_a . While the Frobenius norm of Δ_n depends on the mean vectors $\{\mu_j\}$, the rank of Δ_n is at most $3(s + 1)$ when there are s change points under H_a . Consequently, we can obtain a deterministic rank bound on the shift of $m_n(-\lambda)$ as stated in Lemma 3.2.

LEMMA 3.2. *Let $\tilde{m}_n(-\lambda) = p^{-1} \text{tr}[(n/(n-1)\tilde{S}_n + \lambda I_p)^{-1}]$. Then,*

$$|m_n(-\lambda) - \tilde{m}_n(-\lambda)| \leq \frac{3(s+1)}{p\lambda}, \quad |m'_n(-\lambda) - \tilde{m}'_n(-\lambda)| \leq \frac{3(s+1)}{p\lambda^2}.$$

Moreover, let $\tilde{\Theta}(\lambda)$ and $\tilde{\Gamma}(\lambda)$ be the counterpart of $\hat{\Theta}(\lambda)$ and $\hat{\Gamma}(\lambda)$ when $m_n(-\lambda)$ is replaced by $\tilde{m}_n(-\lambda)$ in (2.4). Then,

$$|\hat{\Theta}(\lambda) - \tilde{\Theta}(\lambda)| \leq \frac{3(s+1)}{p}, \quad |\hat{\Gamma}(\lambda) - \tilde{\Gamma}(\lambda)| \leq \mathcal{K} \frac{3(s+1)}{p},$$

where \mathcal{K} is a constant depending only on γ_n . Consequently, the convergence results in Lemma 3.1 continue to hold under H_a , given that s is fixed.

3.4.2. Power analysis for the single change-point case. We first consider the case $s = 1$ as a benchmark for understanding the power behavior of the proposed test. Under H_a^{SC} , the power is determined by the mean shift $\delta_p = \mu_n - \mu_1$. Denote the power of the proposed decision rule for detecting a single change point at asymptotic size α to be

$$\beta_{\text{sc}}(\lambda, \delta_p) = \mathbb{P}\left(T_{\text{sc}}(\varepsilon, \lambda) > \xi_{\text{sc}}(1 - \alpha, \varepsilon) \mid \delta_p\right).$$

Here, the probability measure $\mathbb{P}(\cdot \mid \delta_p)$ is the distribution of the observations given δ_p .

THEOREM 3.3. *Suppose that Conditions **C1–C5** hold. Under the single change point alternative H_a^{SC} , define*

$$q_p(\lambda, \delta_p) = \sqrt{p} \delta_p^T \mathcal{D}_p(\lambda) \delta_p,$$

where $\mathcal{D}_p(\lambda)$ is the deterministic equivalent in (3.3). If there exist constants $0 < \underline{\mathcal{K}} \leq \bar{\mathcal{K}}$ such that $\underline{\mathcal{K}} \leq q_p(\lambda, \delta_p) \leq \bar{\mathcal{K}}$ for all sufficiently large p , then

$$\beta_{\text{sc}}(\lambda, \delta_p) - \mathbb{P} \left(\sup_{t \in [\varepsilon, 1-\varepsilon]} \left\{ G(0, t, 1) + \gamma_n^{-1} \eta_{\text{sc}}(t) \frac{q_p(\lambda, \delta_p)}{\Gamma_n^{1/2}(\lambda)} \right\} > \xi_{\text{sc}} \right) \longrightarrow 0.$$

Here, $\eta_{\text{sc}}(t) = t(1-t)^{-1}(1-\tilde{t}_1)^2$, if $0 \leq t < \tilde{t}_1$, and $\eta_{\text{sc}}(t) = t^{-1}(1-t)\tilde{t}_1^2$, if $\tilde{t}_1 \leq t \leq 1$.

Theorem 3.3 shows that the local power is asymptotically governed by $q_p(\lambda, \delta_p)/\Gamma_n^{1/2}(\lambda)$ and $\eta_{\text{sc}}(t)$. The former can be interpreted as the asymptotic signal-to-noise ratio (ASNR), while the latter captures the effect of the location of the true change point \tilde{t}_1 .

REMARK 3.1. *Theorem 3.3 shows that the proposed test has non-trivial power in the regime $\sqrt{n}\|\delta_p\|_2^2 \asymp 1$. If instead $\sqrt{n}\|\delta_p\|_2^2 \rightarrow 0$, the power $\beta_{\text{sc}}(\lambda, \delta_p)$ degenerates to the significance level α . On the other hand, if $\sqrt{n}\|\delta_p\|_2^2 \rightarrow \infty$, the power converges to 1.*

Aston and Kirch (2018) introduced the concept of high-dimensional efficiency (HDE), which has been widely used in the power analysis of change point detection methods. Under their framework, the HDE of the proposed test is $\|\delta_p\|_2^2$.

While the power analysis under deterministic local alternatives, characterized by a sequence of deterministic mean shifts, is informative, we now turn to a Bayesian framework referred to as *probability alternatives (PA)*. In this framework, the alternative H_a^{SC} is modeled through a sequence of prior distributions on the mean shift δ_p . An important advantage of the PA framework is its flexibility in incorporating structural information about δ_p . This approach was first proposed in Li et al. (2020b) in the context of two-sample mean testing and was later extended in Li et al. (2020a). In particular, we focus on the following class of prior distributions for δ_p under the alternative hypothesis.

PA-SC. Assume that, under H_a^{SC} , $\delta_p = p^{-3/4} B w$ where B is a $p \times p$ matrix and w is a random vector with independent entries w_i such that $\mathbb{E}w_i = 0$, $\mathbb{E}w_i^2 = 1$ and $\max_i \mathbb{E}|w_i|^4 \leq p^{c_w}$, for some $c_w \in (0, 1)$. Assume that, $\|B\|_2 < \infty$ and $p^{-1} \text{tr}(BB^T) \geq \mathcal{K}$ for some constant $\mathcal{K} > 0$, as $p \rightarrow \infty$.

To better understand **PA-SC**, first observe that δ_p has mean zero and covariance matrix $\mathbf{B} := p^{-3/2} BB^T$. The factor $p^{-3/4}$ provides the scaling under which $\sqrt{n}\|\delta_p\|_2^2 = O_p(1)$, so that the proposed test has non-trivial local power. The framework is quite general, encompassing both dense and sparse alternatives. Representative cases include:

- (I) Dense alternative: the components w_i are i.i.d. $N(0, 1)$;
- (II) Sparse alternative: w_i are i.i.d. following a three-point distribution that assigns probability $(1/2)p^{-c_w}$ to the points $\pm p^{c_w/2}$ and probability $(1-p^{-c_w})$ to 0. If, in addition, $B = I_p$, then δ_p is sparse in the original coordinate system with the degree of sparsity governed by the parameter c_w .

THEOREM 3.4. *Suppose that Conditions **C1–C5** hold. Assume that, under the single change point alternative H_a^{SC} , the mean shift δ_p has prior given by **PA-SC**. Define*

$$(3.6) \quad q_p(\lambda, B) = p^{-1} \text{tr}[\mathcal{D}_p(\lambda) BB^T].$$

Then, for any fixed $\lambda > 0$,

$$\beta_{\text{sc}}(\lambda, \delta_p) - \mathbb{P} \left(\sup_{t \in [\varepsilon, 1-\varepsilon]} \left\{ G(0, t, 1) + \gamma_n^{-1} \eta_{\text{sc}}(t) \frac{q_p(\lambda, B)}{\Gamma_n^{1/2}(\lambda)} \right\} > \xi_{\text{sc}} \right) \xrightarrow{\mathbb{P}_\delta} 0,$$

where the convergence $\xrightarrow{\mathbb{P}_\delta}$ is in probability with respect to the prior distribution of δ_p , and $\eta_{\text{sc}}(t)$ is defined in Theorem 3.3.

Theorem 3.4 shows that the asymptotic power of the proposed test under the **PA** framework is governed by the functions $q_p(\lambda, B)$ and $\eta_{\text{sc}}(t)$. The former characterizes the effect of the covariance matrix \mathbf{B} of δ_p through its interaction with the data covariance matrix Σ_p and the tuning parameter λ . The latter, $\eta_{\text{sc}}(t)$, reflects the effect of the location of the true change point. Notably, no distributional feature of δ_p other than \mathbf{B} and the imposed moment conditions affects the asymptotic power. This implies that the proposed method has the same asymptotic power under dense or sparse alternatives, as long as the covariance structure is the same. It is of interest to compare the proposed method with ℓ_∞ -norm approaches designed for detecting sparse alternatives. We address this comparison in Section 3.4.4.

Importantly, the parameter λ affects the power asymptotically through $q_p(\lambda, B)\Gamma_n^{-1/2}(\lambda)$. We henceforth refer to this product as the asymptotic signal-to-noise ratio (ASNR) under **PA**.

3.4.3. Power analysis for the multiple change-points case. We next consider the general case in which the number of change points s is unknown. For simplicity, we present the analysis only for the scanning set $\mathcal{T}(\varepsilon)$. All results in this section apply directly to the computationally efficient scanning strategy after replacing the scanning set to $\mathcal{T}_*(\varepsilon)$ and replacing the corresponding critical values.

Under H_a , we collect the segment mean vectors across the $(s+1)$ segments into the matrix

$$\mathcal{U} = (\mu_1, \mu_{k_1+1}, \mu_{k_2+1}, \dots, \mu_{k_s+1}) \in \mathbb{R}^{p \times (s+1)}.$$

Notably, when $s = 1$, the mean shift $\delta_p = \mathcal{U}a$, where $a = (1, -1)^T$ is the contrast vector. Denote the power of the proposed decision rule given \mathcal{U} as

$$\beta_{\text{mc}}(\lambda, \mathcal{U}) = \mathbb{P} \left(T_{\text{mc}}(\varepsilon, \lambda) > \xi_{\text{mc}}(1 - \alpha, \varepsilon) \mid \mathcal{U} \right).$$

Here, the probability measure $\mathbb{P}(\cdot \mid \mathcal{U})$ is the distribution of the observations given \mathcal{U} .

For convenience, define the following auxiliary functions. let

$$v_j(x) = \mathbb{1}_{[\tilde{t}_{j-1}, \tilde{t}_j]}(x), \quad x \in [0, 1], \quad j = 1, \dots, s+1,$$

where we set $\tilde{t}_0 = 0$ and $\tilde{t}_{s+1} = 1$. Recall the definition of $u(x; t_1, t_2, t_3)$ in (3.4) and $\kappa(t_1, t_2, t_3)$ in (3.5). We define a $(s+1)$ -vector $\psi(t_1, t_2, t_3)$ for $(t_1, t_2, t_3) \in \mathcal{A}$, whose j th element $\psi_j(t_1, t_2, t_3)$ is

$$\psi_j(t_1, t_2, t_3) = \frac{1}{\sqrt{\kappa(t_1, t_2, t_3)}} \int_0^1 u(x; t_1, t_2, t_3) v_j(x) dx, \quad j = 1, \dots, s+1.$$

THEOREM 3.5. *Suppose that Conditions **C1–C5** hold. Under alternative H_a , assume that there exist constants $0 < \underline{\mathcal{K}} \leq \bar{\mathcal{K}}$ such that*

$$\underline{\mathcal{K}} \leq \sqrt{p} \|\mathcal{U}^T \mathcal{D}_p(\lambda) \mathcal{U}\|_2 \leq \bar{\mathcal{K}}.$$

Then, for any $\lambda > 0$, as $n, p \rightarrow \infty$,

$$\beta_{\text{mc}}(\lambda, \mathcal{U}) - \mathbb{P} \left(\sup_{\mathcal{T}(\varepsilon)} \left\{ G(t_1, t_2, t_3) + \frac{Q_p(t_1, t_2, t_3; \lambda, \mathcal{U})}{\gamma_n \Gamma_n^{1/2}(\lambda)} \right\} > \xi_{\text{mc}}(1 - \alpha, \varepsilon) \right) \rightarrow 0.$$

where $Q_p(t_1, t_2, t_3; \lambda, \mathcal{U}) = \sqrt{p} (\psi(t_1, t_2, t_3))^T \mathcal{U}^T \mathcal{D}_p(\lambda) \mathcal{U} \psi(t_1, t_2, t_3)$.

Similar to the analysis for the single change-point case, we again adopt the **PA** framework, under which the alternative H_a is modeled through a sequence of prior distributions on \mathcal{U} . We focus on the following class of prior distributions with separable covariance structure.

PA-MC. Assume that, under H_a ,

$$\mathcal{U} = p^{-3/4} B W \Omega^T,$$

where W is a $p \times m$ random matrix with independent entries w_{ij} such that $\mathbb{E}w_{ij} = 0$, $\mathbb{E}w_{ij}^2 = 1$, and $\max_{ij} \mathbb{E}|w_{ij}|^4 \leq p^{c_w}$ for some $c_w \in (0, 1)$; B is a $p \times p$ deterministic matrix and Ω is a fixed $(s+1) \times m$ matrix. Here, $m \geq 1$ is any fixed integer. Assume that $\|B\|_2 < \infty$ and $p^{-1} \text{tr}(B B^T) \geq \mathcal{K}$ for some constant $\mathcal{K} > 0$, as $n, p \rightarrow \infty$,

While the matrix B and W play the same role as their counterparts in the single change-point case (denoted by B and w there), the matrix Ω governs the column-wise covariance structure of \mathcal{U} . With different choices of Ω , the model encompasses a variety of structures commonly encountered in many application domains. We give some representative examples. Denote the columns of W as W_j and the columns of \mathcal{U} as $(\mathcal{U})_j$, where $j = 1, \dots, m$.

- (a) Independent: $(\mathcal{U})_j = p^{-3/4} B W_j$. It corresponds to the choice of $m = s+1$ and $\Omega = I_m$.
- (b) Longitudinal: $(\mathcal{U})_j = p^{-3/4} B (W_1 + W_2 j + \dots + W_m j^{m-1})$. It corresponds to the choice of Ω whose (i, j) -th element is i^{j-1} .
- (c) Moving-average: $(\mathcal{U})_j = p^{-3/4} B (\theta W_{j+1} + W_j)$. It corresponds to the choice of Ω whose (i, j) -th element being $\mathbb{1}(i=j) + \theta \mathbb{1}(j-i=1)$.

THEOREM 3.6. *Suppose that Conditions **C1–C5** hold. Assume that, under the alternative H_a , the matrix \mathcal{U} has a prior given by **PA-MC**. Define*

$$q_p(\lambda, B) = p^{-1} \text{tr}(\mathcal{D}_p(\lambda) B B^T).$$

Then, for any fixed $\lambda > 0$,

$$(3.7) \quad \beta_{\text{mc}}(\lambda, \mathcal{U}) - \mathbb{P} \left(\sup_{\mathcal{T}(\varepsilon)} \left\{ G(t_1, t_2, t_3) + \frac{q_p(\lambda, B)}{\gamma_n \Gamma_n^{-1/2}(\lambda)} \left\| \Omega^T \psi(t_1, t_2, t_3) \right\|_2^2 \right\} > \xi_{\text{mc}}(1 - \alpha, \varepsilon) \right) \xrightarrow{\mathbb{P}_{\mathcal{U}}} 0,$$

where the convergence $\xrightarrow{\mathbb{P}_{\mathcal{U}}}$ is in probability with respect to the prior distribution of \mathcal{U} .

Theorem 3.6 indicates that under the separable covariance structure, the row-wise covariance $\mathbf{B} := p^{-3/2} B B^T$ affects the asymptotic power through $q_p(\lambda, B)$, interacting with the data covariance matrix Σ_p and the parameter λ . The column-wise covariance $\Omega \Omega^T$ interacts with the true change-point locations through the Euclidean norm of $\Omega^T \psi(t_1, t_2, t_3)$. No distributional features of W other than \mathbf{B} and the imposed moment conditions affect the asymptotic power, indicating that the proposed method has the same asymptotic power under dense or sparse alternatives.

Again, similar to the single change-point case, the parameter λ affects the asymptotic power through $q_p(\lambda, B) \Gamma_n^{-1/2}(\lambda)$, referred to as the ASNR.

3.4.4. Power Comparison. In this section, we analytically compare the proposed tests with other prevailing testing strategies in the literature under the simple yet representative single change-point setting. Our focus is on the ℓ_2 -norm approaches (Zhang et al., 2010; Wang et al., 2022; Horváth and Hušková, 2012) designed for detecting dense alternatives and the ℓ_∞ -norm approaches (Jiřák, 2012; Yu and Chen, 2021) designed for detecting sparse alternatives.

In particular, define

$$\tilde{C}_\infty(t_1, t_2, t_3) = \frac{1}{k(t_3) - k(t_2)} \sum_{j=k(t_2)}^{k(t_3)-1} X_j - \frac{1}{k(t_2) - k(t_1)} \sum_{j=k(t_1)}^{k(t_2)-1} X_j.$$

Notably, for any fixed set of observations, $\tilde{C}_\infty(t_1, t_2, t_3) = \lim_{\lambda \rightarrow \infty} \lambda^{1/2} C_\lambda(t_1, t_2, t_3)$.

Although they differ in some details, the ℓ_∞ -norm approaches typically consider testing the hypothesis H_0 using

$$(3.8) \quad \max_{t \in [\varepsilon, 1-\varepsilon]} \|\tilde{C}_\infty(0, t, 1)\|_\infty \quad (\text{SC}), \quad \max_{(t_1, t_2, t_3) \in \mathcal{T}(\varepsilon)} \|\tilde{C}_\infty(t_1, t_2, t_3)\|_\infty \quad (\text{MC}),$$

while the ℓ_2 -norm approaches typically consider testing the hypothesis H_0 using

$$(3.9) \quad \max_{t \in [\varepsilon, 1-\varepsilon]} \|\tilde{C}_\infty(0, t, 1)\|_2^2 \quad (\text{SC}), \quad \max_{(t_1, t_2, t_3) \in \mathcal{T}(\varepsilon)} \|\tilde{C}_\infty(t_1, t_2, t_3)\|_2^2 \quad (\text{MC}).$$

In the SC formulation only the single-split contrast $\tilde{C}_\infty(0, t, 1)$ enters because the alternative posits a single change point; the MC formulation scans the full triple set $\mathcal{T}(\varepsilon)$ to accommodate an unknown number of change points.

It is worth mentioning that the U-statistic-based method of Wang et al. (2022) exploits the principle of self-normalization proposed in Shao (2010). Specifically, they remove the squared terms in $\|\tilde{C}_\infty(0, t, 1)\|_2^2$ and retain only the cross-product terms. The resulting statistic has a pivotal limiting distribution that is free from Σ_p . The test is expected to be stable even in an ultra-high-dimensional regime where $p/n \rightarrow \infty$. When p is comparable to n , we expect the performance of the method in Wang et al. (2022) to be close to those ℓ_2 -norm approaches. Such a close relationship between U-statistic-based tests and ℓ_2 -norm tests has been observed in the literature; see, for example, Li et al. (2020b).

A second self-normalized procedure is the test of Zhang and Lavitas (2018), which uses a global ratio statistic. Their statistic is

$$(3.10) \quad \sup_{0 < t < 1} \frac{p^{-1} N(0, t, 1) \|\tilde{C}_\infty(0, t, 1)\|_2^2}{G_n}, \quad G_n = \frac{1}{n^2} \sum_{i=1}^{n-1} \|U_i\|_2^2, \quad (\text{SC})$$

where $U_i = \sum_{t=1}^i (X_t - \bar{X})$. In the MC setting, they propose to search over all possible triples of the form $(0, t_2, t_3)$ and $(t_1, t_2, 1)$. The ratio construction cancels the leading dependence on Σ_p and yields an asymptotically pivotal limit without requiring estimation of Σ_p .

To compare the proposed method with the ℓ_∞ -norm procedures, we work within the **PA** framework equipped with the sparse prior specified in case (II) (see Section 3.4.2), where the parameter c_w controls the degree of sparsity. For simplicity, let $B = \Sigma_p = I_p$ and assume the observations are normal. Under this setup, the proposed test has nontrivial asymptotic power that is free from c_w , as shown in Theorem 3.4.

As for the ℓ_∞ -norm approaches, the statistic in (3.8) under H_0 is of order $O_p(\sqrt{\log(pn)/n})$, or equivalently $O_p(\sqrt{\log(n)/n})$ when $p \asymp n$ as in C2. Therefore, these tests have overwhelming power if the mean shift satisfies $\|\delta_p\|_\infty \gg O_p(\sqrt{\log(n)/n})$, but exhibit degenerate power if $\|\delta_p\|_\infty \ll O_p(\sqrt{\log(p)/p})$. The magnitude of $\|\delta_p\|_\infty$ is governed by c_w . Indeed, if $c_w \in (0, 1/2)$, corresponding to a low sparsity level,

$$\|\delta_p\|_\infty = O_p(p^{-3/4} p^{c_w/2}) \ll p^{-1/2} \ll \sqrt{\log(p)/p},$$

If $c_w \in (1/2, 1)$, which corresponds to a high sparsity level,

$$\|\delta_p\|_\infty = O_p(p^{-3/4} p^{c_w/2}) \gg \sqrt{\log(p)/p}.$$

It indicates that the proposed method is expected to outperform ℓ_∞ -norm approaches for detecting dense alternatives, but to be less efficient for detecting sparse alternatives. The phase transition occurs at the regime $\|\delta_p\|_\infty/\|\delta_p\|_2 \asymp O_p(n^{-1/4}\sqrt{\log(n)})$.

To compare the proposed method with the ℓ_2 -norm approaches, we note that the latter can be viewed as the limiting case of the proposed method when $\lambda \rightarrow \infty$, due to the relationship between \tilde{C}_∞ and C_λ . Indeed, for any fixed set of observations, as $\lambda \rightarrow \infty$,

$$\frac{p^{-1}\lambda V_\lambda(t_1, t_2, t_3) - \lambda\Theta(\lambda)}{\sqrt{\lambda^2\Gamma(\lambda)}} \rightarrow \frac{p^{-1}\|\tilde{C}_\infty(t_1, t_2, t_3)\|_2^2 - \mathfrak{M}_1}{\sqrt{2\mathfrak{M}_2}},$$

where \mathfrak{M}_j is the first and second moments of the PSD H_p ; Namely, $\mathfrak{M}_j = \int \tau^j dH_p(\tau)$, $j = 1, 2$. Therefore, under **PA**, the asymptotic power formula shown in Theorem 3.4 also applies to the ℓ_2 -norm approaches when the ASNR $q_p(\lambda)\Gamma_n^{-1/2}(\lambda)$ is replaced by its limit as $\lambda \rightarrow \infty$, providing existence. In particular, as $\lambda \rightarrow \infty$, we have

$$q_p(\lambda)\Gamma_p^{-1/2}(\lambda) - \frac{p^{-1}\text{tr}(BB^T)}{\sqrt{2p^{-1}\text{tr}(\Sigma_p^2)}} \rightarrow 0.$$

The power comparison between the proposed method and the ℓ_2 -norm approaches therefore depends on the population covariance structure Σ_p , the covariance structure \mathbf{B} , and the choice of λ . In particular, if $q_p(\lambda)\Gamma_n^{-1/2}(\lambda)$ attains its maximum at some $\lambda_0 < \infty$, the proposed method is expected to outperform the ℓ_2 -norm approaches when $\lambda \approx \lambda_0$. Otherwise, if $q_p(\lambda)\Gamma_n^{-1/2}(\lambda)$ achieves its maximum only in the limit $\lambda \rightarrow \infty$, the ℓ_2 -norm approach is expected to outperform the proposed method at any finite choice of λ .

While a full analytical comparison among these methods under general \mathbf{B} is challenging, we show that the ASNR is maximized at small values of λ under a class of models for \mathbf{B} in which \mathbf{B} is a linear function of Σ_p . Further details are provided in Section 4. In addition, we investigate numerically the behavior of the ASNR under a range of covariance models commonly used in practice. Across all models considered, the estimated ASNR is maximized at small values of λ . This observation supports the use of small regularization parameters in the proposed procedure.

4. Selection of the Regularization Parameter. In this section, we discuss the problem of selecting λ . Our analysis is conducted under the **PA** model introduced in Section 3.4. While the strategy is presented for detecting multiple change points using the test statistic $T_{\text{mc}}(\varepsilon, \lambda)$, the same strategy applies to the single change-point case and to the computationally efficient test $T_{\text{mc}}^*(\varepsilon, \lambda)$. Throughout the analysis, we assume that a prespecified range for λ , say $[\underline{\lambda}, \bar{\lambda}]$, is given. The parameter ε and the significance level α are treated as fixed and are therefore suppressed from the subsequent notation.

4.1. *Bayesian Decision Theory.* Consider the class of tests

$$\mathfrak{T} = \left\{ \mathbb{I}(T_{\text{mc}}(\lambda) > \xi_{\text{mc}}) : \lambda \in [\underline{\lambda}, \bar{\lambda}] \right\}.$$

For any given **PA** prior model on \mathcal{U} , say \mathcal{P} , we define the *asymptotic Bayes risk* of the proposed test with parameter λ with respect to the prior \mathcal{P} as

$$(4.1) \quad R(\lambda, \mathcal{P}) = \limsup_{n, p \rightarrow \infty} (1 - \mathbb{E}_{\mathcal{P}}[\beta_{\text{mc}}(\lambda, \mathcal{U})]) = 1 - \liminf_{n, p \rightarrow \infty} \mathbb{E}_{\mathcal{P}}[\beta_{\text{mc}}(\lambda, \mathcal{U})].$$

Here, $\mathbb{E}_{\mathcal{P}}$ denotes expectation taken with respect to the prior \mathcal{P} .

Naturally, if \mathcal{P} is given, we choose λ to minimize this risk function. This choice leads to the asymptotic Bayes decision rule associated with the prior \mathcal{P} . Namely, let

$$(4.2) \quad \lambda_b(\mathcal{P}) = \arg \min_{\lambda \in [\underline{\lambda}, \bar{\lambda}]} R(\lambda, \mathcal{P}).$$

Then, the decision rule $\mathbb{I}(T_{\text{mc}}(\lambda_b(\mathcal{P})) > \xi_{\text{mc}})$ is the corresponding *asymptotic Bayes test* with respect to the prior \mathcal{P} within the class \mathfrak{F} .

Notably, under **PA**, Theorem 3.6 shows that the parameter λ affects the asymptotic risk only through the ASNR $q_p(\lambda, B)\Gamma_n^{-1/2}(\lambda)$. Consequently, maximizing (minimizing) the risk function is equivalent to minimizing (maximizing) the ASNR. The latter depends on the prior model \mathcal{P} only through the row-wise covariance matrix $\mathbf{B} = p^{-3/2}BB^T$. In other words, two different priors lead to the same asymptotic Bayes test if they share the same \mathbf{B} . For this reason, we henceforth fix the distribution of W and the matrix Ω in **PA**. The prior \mathcal{P} is then solely determined by \mathbf{B} , and we write $\mathcal{P} = \mathcal{P}(\mathbf{B})$.

4.2. Minimality. In practice, rather than a particular choice of the prior, we may consider a collection of such priors. In such situations, a strategy is needed to synthesize the information they provide and enhance the robustness against prior misspecification. We further consider a procedure for selecting the regularization parameter based on the principle of minimaxity. To this end, consider a family of matrices \mathbf{B} indexed by a parameter $\underline{\theta} \in \mathcal{E}$, denoted by $\mathbf{B}_{\underline{\theta}}$, under the constraint

$$(4.3) \quad \sqrt{p} \text{tr}(\mathbf{B}_{\underline{\theta}}) = \mathcal{K}, \quad \text{for all } \underline{\theta} \in \mathcal{E}.$$

Here, $\mathcal{K} > 0$ is a constant and \mathcal{E} is a compact index set. Condition (4.3) ensures that the expected signal strength $\mathbb{E}_{\mathcal{P}(\mathbf{B}_{\underline{\theta}})} \|\mathcal{U}\|_F^2$ remains the same for all $\underline{\theta} \in \mathcal{E}$. Without loss of generality, we set $\mathcal{K} = 1$. We denote the family of priors determined by $\mathbf{B}_{\underline{\theta}}$, $\underline{\theta} \in \mathcal{E}$, to be

$$(4.4) \quad \mathfrak{F} = \{\mathcal{P}(\mathbf{B}_{\underline{\theta}}), \underline{\theta} \in \mathcal{E} : \sqrt{p} \text{tr}(\mathbf{B}_{\underline{\theta}}) = 1\}.$$

We say that the decision rule $\mathbb{I}(T_{\text{mc}}(\lambda_*) > \xi_{\text{mc}})$ is *asymptotically minimax* with respect to the family \mathfrak{F} if

$$\lambda_* = \arg \min_{\lambda \in [\underline{\lambda}, \bar{\lambda}]} \sup_{\underline{\theta} \in \mathcal{E}} R(\lambda, \mathcal{P}(\mathbf{B}_{\underline{\theta}})) = \arg \max_{\lambda \in [\underline{\lambda}, \bar{\lambda}]} \inf_{\underline{\theta} \in \mathcal{E}} \frac{q_p(\lambda, \underline{\theta})}{\Gamma_n^{1/2}(\lambda)}.$$

Here, $q_p(\lambda, \underline{\theta})$ denotes $q_p(\lambda, B)$ evaluated at B satisfying $p^{-3/2}BB^T = \mathbf{B}_{\underline{\theta}}$. We henceforth refer to λ_* as the *minimax choice* of λ .

4.3. Practical Considerations. To implement the proposed strategies, a consistent estimator of $q_p(\lambda, \underline{\theta})$ is required. To this end, we consider two scenarios. First, when $\mathbf{B}_{\underline{\theta}}$ is specified, we estimate $q_p(\lambda, \underline{\theta})$ by

$$(4.5) \quad \hat{q}(\lambda, \underline{\theta}) = \frac{1}{p} \text{tr}[(S_n + \lambda I_p)^{-1} \mathbf{B}_{\underline{\theta}}], \quad \underline{\theta} \in \mathcal{E}.$$

The consistency of $\hat{q}(\lambda, \underline{\theta})$ is well established in the RMT literature and is therefore omitted. We then propose to select λ according to the Bayes principle by

$$\hat{\lambda}_b(\mathcal{P}(\mathbf{B}_{\underline{\theta}})) = \arg \max_{\lambda \in [\underline{\lambda}, \bar{\lambda}]} \frac{\hat{q}(\lambda, \underline{\theta})}{\hat{\Gamma}^{1/2}(\lambda)}.$$

Moreover, given a family of priors \mathfrak{F} in the form of (4.4), we propose to select λ according to the minimax principle by

$$\hat{\lambda}_* = \arg \max_{\lambda \in [\underline{\lambda}, \bar{\lambda}]} \inf_{\underline{\theta} \in \mathcal{E}} \frac{\hat{q}(\lambda, \underline{\theta})}{\hat{\Gamma}^{1/2}(\lambda)}.$$

This scenario typically arises when additional structural information about the signal is available. For example, under a stationary autocovariance assumption, the matrix \mathbf{B}_θ may be specified as a Toeplitz covariance matrix. In contrast, when no such structural information is available, specifying a high-dimensional positive definite matrix \mathbf{B}_θ becomes challenging.

We now turn to the second scenario. Motivated by Li et al. (2020b), we adopt a linear alternative framework in which \mathbf{B}_θ is restricted to be a linear function of Σ_p . Specifically, we consider the family

$$(4.6) \quad \mathfrak{P}_{\text{LN}} = \{ \mathcal{P}(\mathbf{B}_\theta) : \mathbf{B}_\theta = \theta_1 I_p + \theta_2 \Sigma_p, \theta_1, \theta_2 \geq 0, p^{-1} \text{tr}(\mathbf{B}_\theta) = 1 \}.$$

Under this scenario, \mathbf{B}_θ is specified by the coefficients $\underline{\theta} = (\theta_1, \theta_2)$ subject to the unknown population covariance Σ_p . This family admits a simple and intuitive interpretation of the structure of \mathcal{U} . In particular, $\theta_2 = 0$ corresponds to a prior under which the rows of \mathcal{U} are independent and share a common column-wise covariance, suggesting that the signal is evenly spread across all coordinates. In contrast, a large value of θ_2 concentrates the signal increasingly along the leading eigendirections of Σ_p .

LEMMA 4.1. *Suppose that Conditions C1–C5 hold. Let $\mathbf{B}_\theta \in \mathfrak{P}_{\text{LN}}$. Consider $\lambda \in [\underline{\lambda}, \bar{\lambda}]$. The following results hold.*

- (i) *For any fixed $\lambda > 0$, the ASNR $q_p(\lambda, \underline{\theta}) \Gamma_n^{-1/2}(\lambda)$ is strictly decreasing in θ_2 .*
- (ii) *For any fixed $\underline{\theta}$, the ASNR $q_p(\lambda, \underline{\theta}) \Gamma_n^{-1/2}(\lambda)$ is strictly decreasing in λ .*

Consequently, for any Σ_p and any fixed $\mathbf{B}_\theta \in \mathfrak{P}_{\text{LN}}$, the asymptotic Bayes test is attained at $\lambda = \underline{\lambda}$. Moreover, the asymptotic minimax choice of λ with respect to \mathfrak{P}_{LN} is also given by $\underline{\lambda}$.

It is also of interest to study analytically the minimax choice of λ under the first scenario, for example, when \mathbf{B}_θ follows a given parametric model. However, such an analysis appears intractable in general, due to the absence of a closed-form expression for $\sqrt{p} \text{tr}[\mathcal{D}_p(\lambda) \mathbf{B}_\theta]$, which depends on the projection of \mathbf{B}_θ onto the eigenspaces of Σ_p .

We therefore conduct numerical experiments to investigate the behavior of the ASNR under representative covariance models. It is found that across a broad range of models considered, the minimax choice is attained at the lower bound $\underline{\lambda}$, although a theoretical justification is not currently available. This empirical evidence suggests that selecting a small value of λ provides a reasonable practical guideline. While any $\lambda > 0$ is theoretically admissible in our analysis, from a practical perspective λ should not be chosen too small in order to ensure the stability of $(S_n + \lambda I_p)^{-1}$. In our implementation, we recommend taking

$$\underline{\lambda} \approx 0.01 p^{-1} \text{tr}(S_n).$$

Lastly, when λ is selected in a data-driven manner, a potential concern arises from the “double-dipping” issue, since the same dataset is used both to select λ and to perform the test. While we have derived the asymptotic distribution of the proposed test statistics for a fixed λ , the data-driven choice $\hat{\lambda}$ introduces additional randomness that may, in principle, affect the asymptotic behavior. To mitigate the fluctuation of $\hat{\lambda}$, we propose restricting the search to a finite discrete subset of $[\underline{\lambda}, \bar{\lambda}]$. This discretization is not expected to incur a substantial loss of efficiency, owing to the smooth dependence of the test statistic on λ .

5. Simulation Studies. In this section, we evaluate the performance of the proposed methods and compare them with representative existing approaches via Monte Carlo experiments. We focus on the data-generating model (1.1), where Z_j are standard normal.

We consider four models for Σ_p in (1.1): (i) (ID) $\Sigma_p = I_p$; (ii) (Toeplitz) Σ_p is a Toeplitz matrix with (i, j) -th entry $0.3^{|i-j|}$; (iii) (Poly Decay) The eigenvalues τ_j of Σ_p decay polynomially as $\tau_j = 0.01 + (p - j + 0.1)^2$; (iv) (Exp Decay) The eigenvalues τ_j of Σ_p decay exponentially as $\tau_j = \exp(-3j/p)$. For all models, Σ_p is further scaled so that $\text{tr}(\Sigma_p) = p$. The Exp Decay model represents a challenging setting in which the spectrum of Σ_p contains several dominant spikes, corresponding to a covariance matrix that is nearly low rank.

For the proposed tests, we set the trimming parameter $\varepsilon = 0.1$. The following competing methods are included in the comparison.

- **L_2^2 -CUSUM.** The test statistics are given by (3.9) under the SC and MC settings. This method can be viewed as the limiting case of the proposed procedure as $\lambda \rightarrow \infty$.
- **L_∞ -CUSUM.** The same scanning strategy as the L_2^2 -CUSUM, but with the squared ℓ_2 -norm replaced by the (unstandardized) ℓ_∞ -norm given in (3.8). This statistic is the natural counterpart to L_2^2 -CUSUM under sparse alternatives and serves as a benchmark for the sparse signal models.
- **Zhang–Lavitas.** The test statistics are given by (3.10) proposed by Zhang and Lavitas (2018). The method is feasible and free of Monte Carlo calibration, but achieves pivotality through self-normalization rather than ridge regularization. For a fair comparison, we implement this method using the scanning strategy proposed in the present paper instead of their original proposal.

Because the L_2^2 - and L_∞ -CUSUM statistics are not asymptotically pivotal in the high-dimensional regime, their critical values are obtained via Monte Carlo simulation under each (Σ_p, p, n) configuration to attain the nominal significance level. This calibration removes any Type I error advantage and ensures that the power comparison reflects the discriminating ability of the test statistic itself.

5.1. Null Validation. We assess the null distribution of the proposed test statistics under H_0 . We consider $n = 200$ and $\gamma = p/n \in \{0.5, 1, 2\}$. We fix $\lambda/\gamma \in \{0.1, 0.2\}$. The empirical sizes at the nominal level 5% are reported in Table

TABLE 5.1
Empirical sizes $\times 100\%$ of the proposed test statistics at nominal level $\alpha = 0.05$.

$n = 200$	λ/γ	$\Sigma_p = \text{Identity}$			$\Sigma_p = \text{Toeplitz}$			$\Sigma_p = \text{Poly Decay}$			$\Sigma_p = \text{Exp Decay}$		
		$p = 100$	$p = 200$	$p = 400$	$p = 100$	$p = 200$	$p = 400$	$p = 100$	$p = 200$	$p = 400$	$p = 100$	$p = 200$	$p = 400$
T_{sc}	0.1	5.26	2.85	5.62	5.34	2.87	5.83	6.24	3.84	3.96	5.80	3.49	4.90
	0.2	5.56	3.67	4.41	5.49	3.73	4.71	6.59	4.67	4.11	6.22	4.47	4.71
T_{mc}	0.1	5.35	1.45	4.65	5.69	1.89	4.93	6.86	3.18	2.85	5.83	2.61	4.23
	0.2	5.59	2.41	3.87	6.03	3.02	4.17	7.33	4.09	3.45	6.46	3.99	4.20

The results confirm the validity of the proposed Gaussian process approximation to the finite-sample distributions of T_{sc} and T_{mc} across a range of covariance settings. In general, the empirical sizes of T_{mc} are slightly inflated, which can be attributed to the increased variability induced by the larger scanning set.

5.2. Power Comparison. We evaluate empirical power across all four covariance settings introduced at the start of Section 5, with $p \in \{100, 200, 400\}$ and $n = 3p$. Other aspect ratios p/n are also investigated, but not reported, as they show similar patterns. The nominal significance level is $\alpha = 0.05$, and rejection rates are based on 500 Monte Carlo replications. The proposed tests were run at two tuning levels, $\lambda/\gamma \in \{0.1, 0.2\}$; since the two produce nearly identical power, we report only $\lambda/\gamma = 0.1$.

We study three signal models for the jump vector $\delta \in \mathbb{R}^p$:

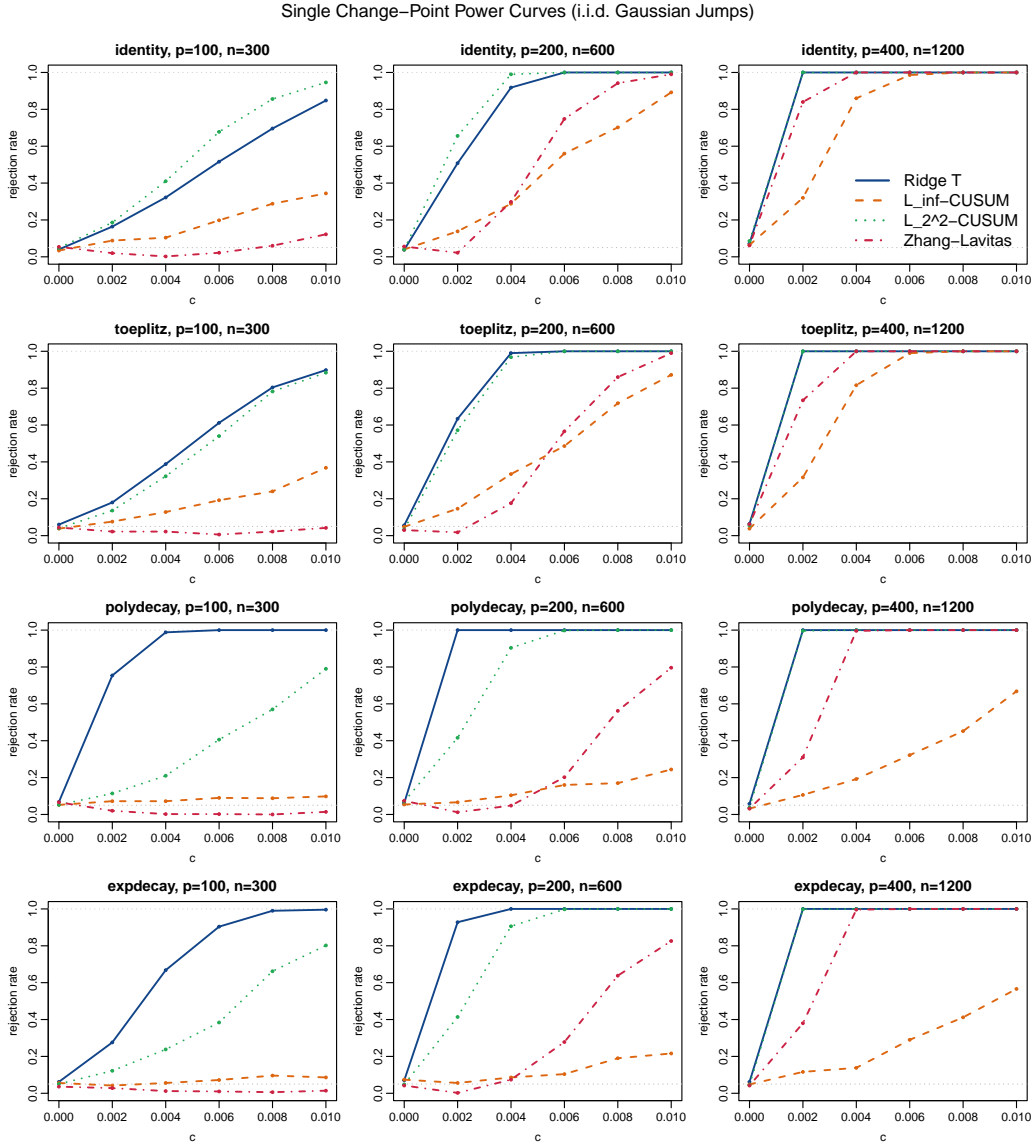


Fig 5.1: Single change-point power against the i.i.d. Gaussian alternative with change point at $k_0 = 0.5n$ and ridge tuning $\lambda/\gamma = 0.1$.

- **i.i.d. Gaussian.** $\delta \sim N(0, cI_p)$, dense in the original coordinates with homoscedastic per-coordinate signal.
- **Σ_p -correlated Gaussian.** $\delta \sim N(0, c\Sigma_p)$, so the whitened signal $\Sigma_p^{-1/2}\delta$ is i.i.d. $N(0, cI_p)$.
- **Sparse.** Three randomly chosen coordinates are set to $\pm 5c$ with random signs and the remaining $(p-3)$ entries are zero. The fixed sparsity level $s = 3$ ensures that the alternative is genuinely sparse at every p .

The parameter c controls the signal strength and the power of the tests against c is displayed.

Single change-point. We test against a single change at $k_0 = \lfloor 0.5n \rfloor$. Figures 5.1, 5.2, and 5.3 report the empirical power under all settings.

Single Change-Point Power Curves (Sigma-Correlated Gaussian Jumps)

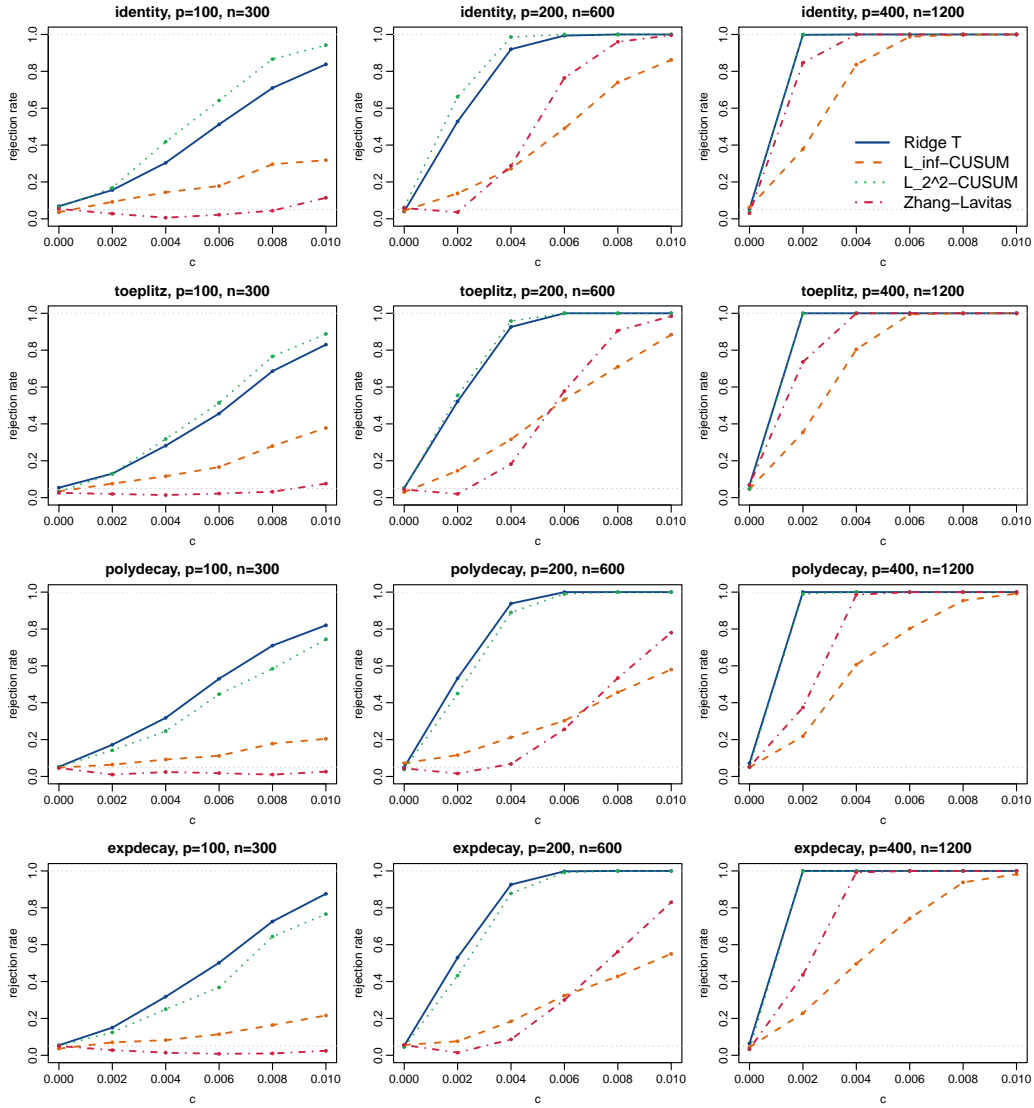


Fig 5.2: Single change-point power against the Σ_p -correlated Gaussian alternative with change point at $k_0 = 0.5n$ and ridge tuning $\lambda/\gamma = 0.1$.

The simulation results show that, across all configurations considered, the proposed ridge-based test attains power comparable to the best-performing competing method, except in settings with sparse mean shifts and $\Sigma_p = I_p$. This provides evidence that the proposed procedure adapts well to different signal structures and covariance patterns, distinguishing it from existing methods.

When $\Sigma_p = I_p$ or when the mean shift μ is aligned with the covariance structure of Σ_p , the L_2^2 -CUSUM procedure is a strong competitor. In particular, when $\Sigma_p = I_p$, L_2^2 -CUSUM is expected to perform best, as it effectively uses the true covariance structure. When μ is Σ_p -correlated, the proposed method rescales the coordinates using data-driven variance estimates, thereby adapting to the underlying covariance structure, whereas the L_2^2 -CUSUM statistic aggregates the signal without such scaling.

Single Change-Point Power Curves (Sparse Jumps)

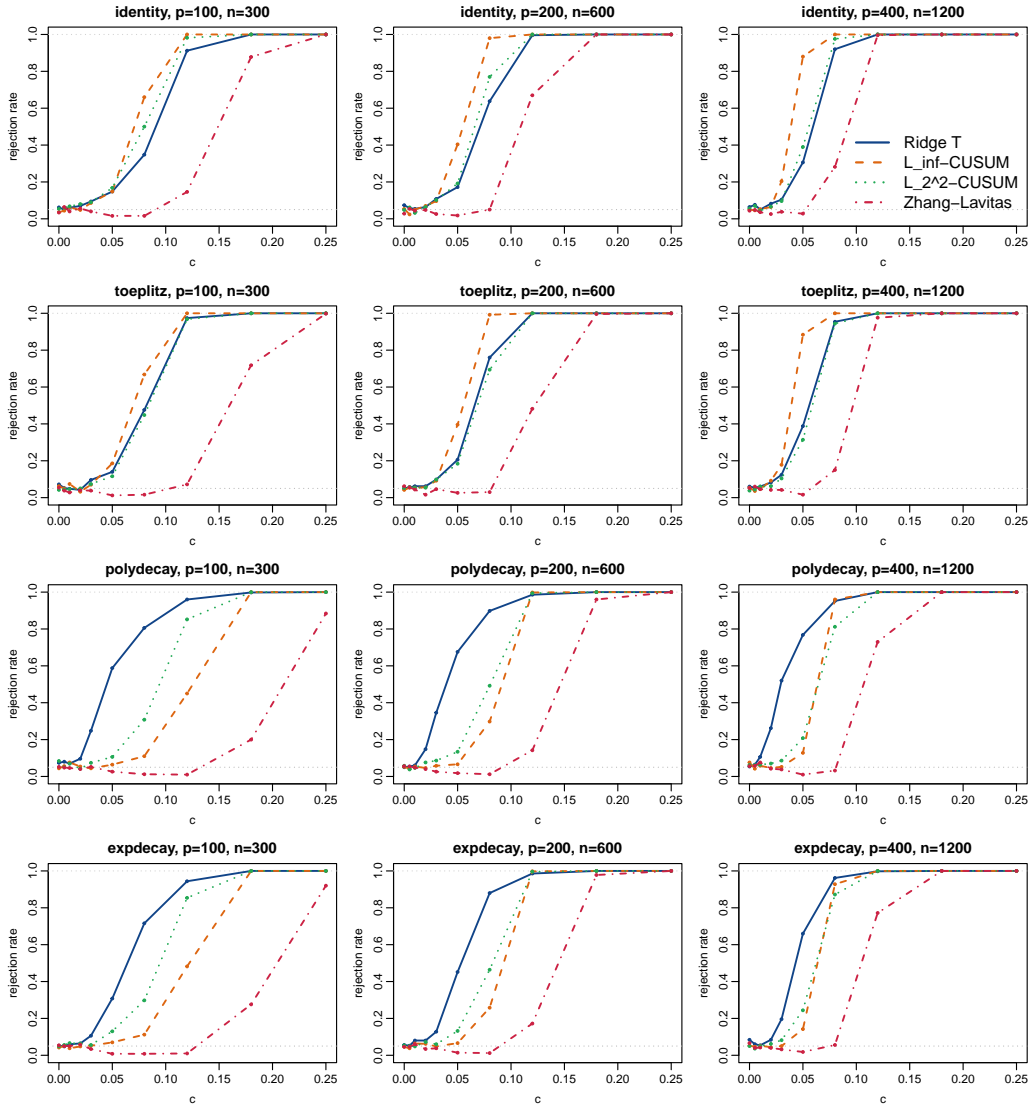


Fig 5.3: Single change-point power against the sparse alternative with $s = 3$ nonzero coordinates of magnitude $\pm 5c$, change point at $k_0 = 0.5n$ and ridge tuning $\lambda/\gamma = 0.1$.

When the jump δ is sparse, the L_∞ -CUSUM procedure is a strong competitor, especially under homoscedastic covariance structures. However, sparsity alone does not guarantee superior performance. Under heteroscedastic Σ_p , the null threshold of the L_∞ -CUSUM is driven by the largest noise variance, which can adversely affect its power.

Lastly, Zhang-Lavitas is dominated in every configuration and is the slowest method to ramp up at every p in our grid, suggesting that its self-normalization machinery requires substantially larger sample sizes than the other procedures to extract power from a fixed signal.

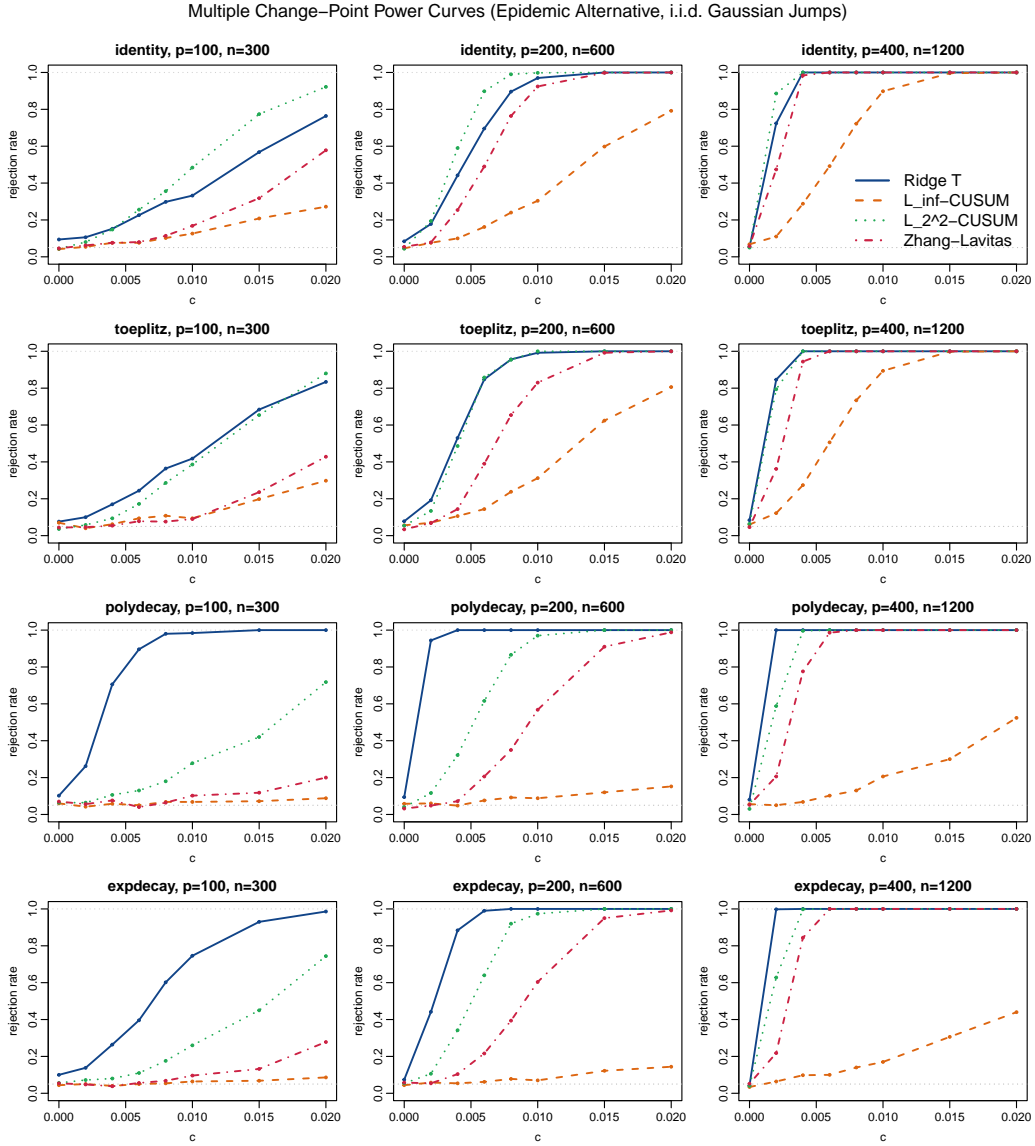


Fig 5.4: Multiple change-point power against the i.i.d. Gaussian alternative under the epidemic configuration $(\tau_1, \tau_2) = (0.35, 0.65)$ with $\lambda/\gamma = 0.1$.

Multiple change-points (epidemic alternative). We test against the epidemic alternative

$$\mu_t = \begin{cases} 0, & t \leq \tau_1 n, \\ \delta, & \tau_1 n < t \leq \tau_2 n, \\ 0, & t > \tau_2 n, \end{cases}$$

with $(\tau_1, \tau_2) = (0.35, 0.65)$. Figures 5.4, 5.5, and 5.6 report the results.

The epidemic setting confirms the qualitative findings of the single change-point analysis: the proposed ridge-based test is the only feasible procedure that delivers nontrivial power across all combinations of signal model and covariance structure. Among the feasible competitors, only the proposed test and Zhang-Lavitas enjoy asymptotically pivotal null distributions whose critical values can be obtained without simulation-based calibration; the L_2^2 - and

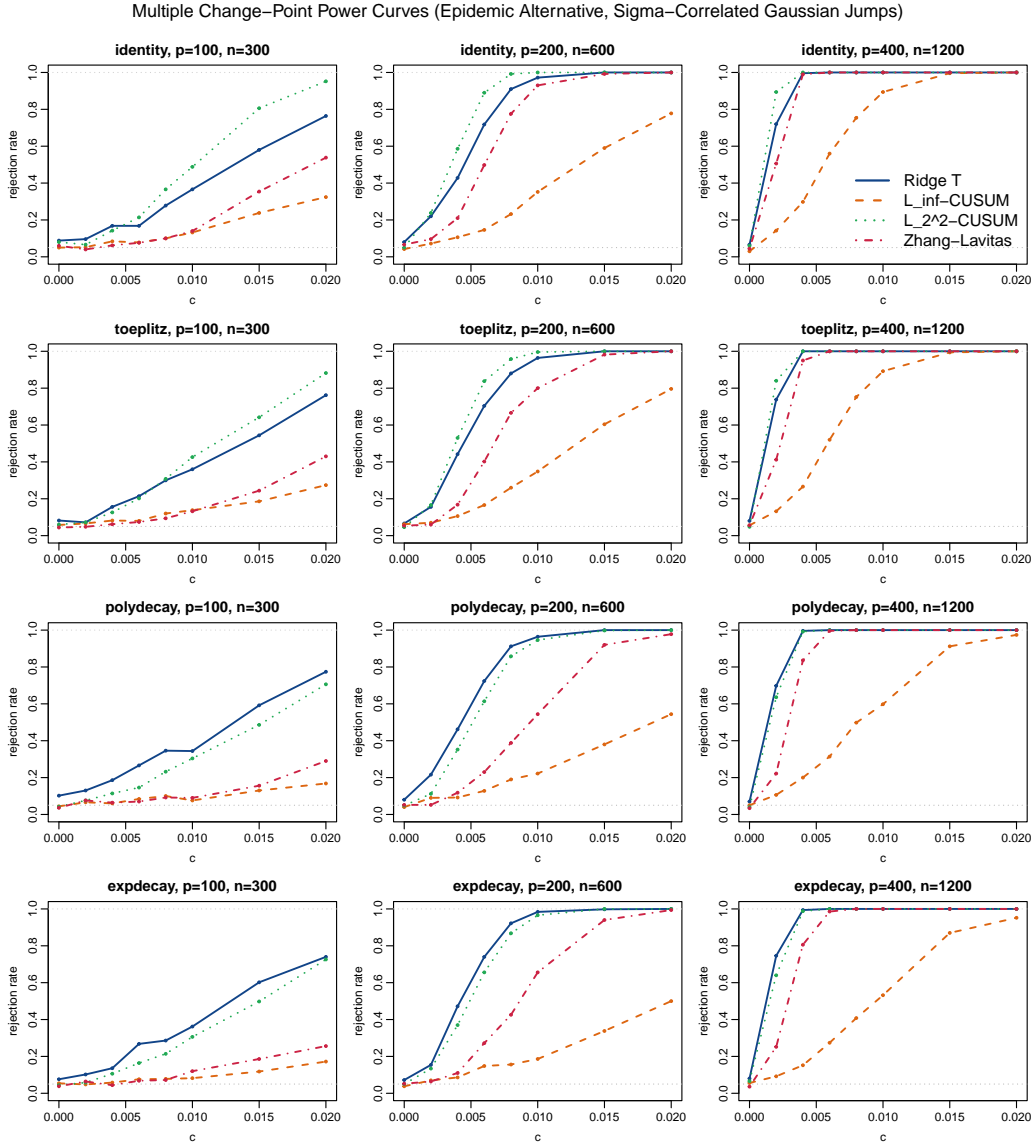


Fig 5.5: Multiple change-point power against the Σ_p -correlated Gaussian alternative under the epidemic configuration with $\lambda/\gamma = 0.1$.

L_∞ -CUSUM both require Monte Carlo calibration under each new covariance. Despite sharing this practical advantage with the proposed test, Zhang-Lavitas's power gap is sharper in the epidemic setting than in the single change-point case, reflecting the additional difficulty self-normalization faces under multi-segment alternatives.

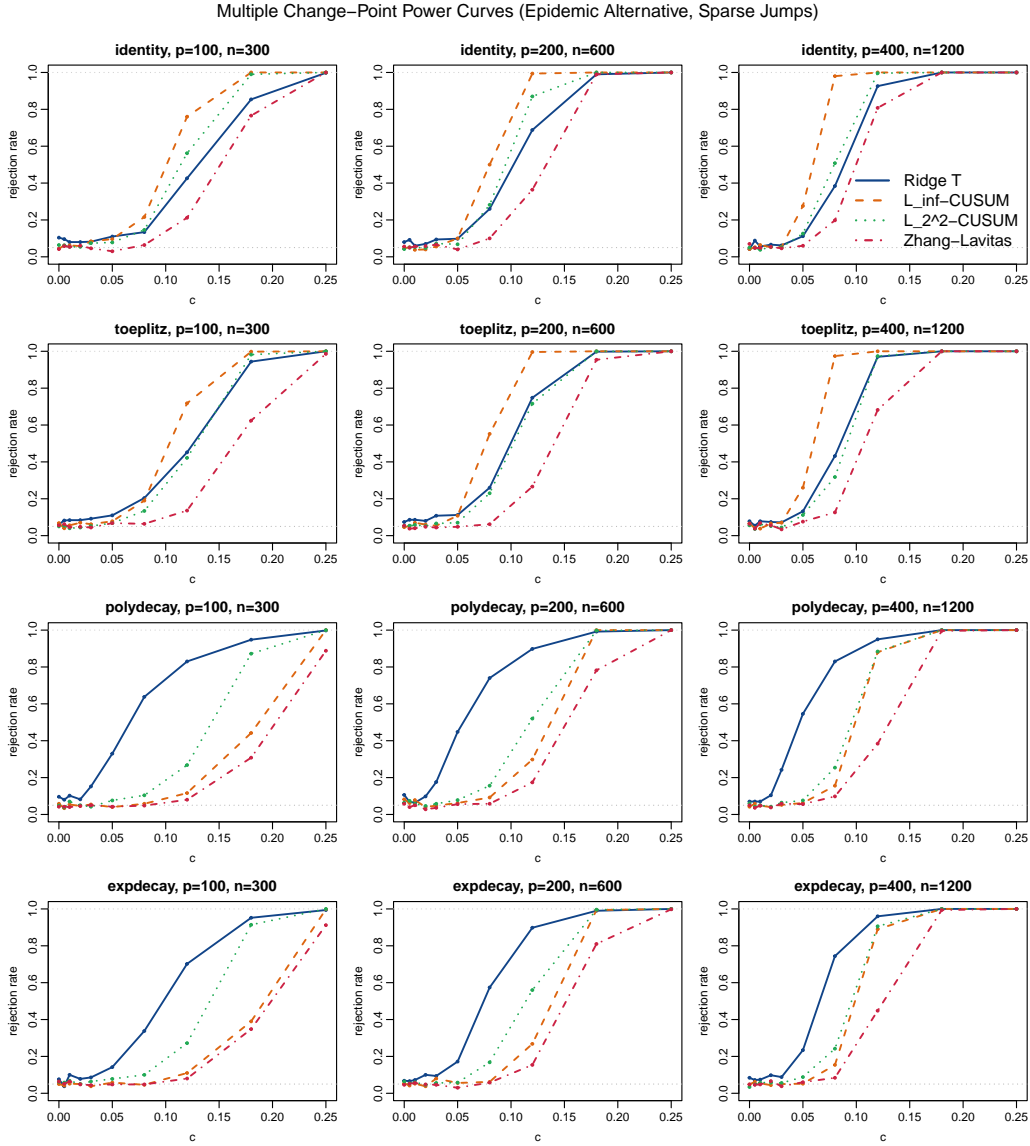


Fig 5.6: Multiple change-point power against the sparse alternative ($s = 3$ nonzero coordinates of magnitude $\pm 5c$) under the epidemic configuration with $\lambda/\gamma = 0.1$.

6. Real Data. We apply the proposed Ridge tests and the feasible competitors to a panel of daily stock returns from constituents of the S&P 500 index. We select $p = 92$ stocks that have been long-standing members of the S&P 500 and have complete daily price data from January 2007 through December 2025, spanning all eleven GICS sectors (technology, financials, healthcare, consumer discretionary and staples, energy, industrials, utilities, real estate, materials, and communication services). Adjusted closing prices are obtained from Yahoo Finance and converted to daily log-returns, yielding a panel of $n = 4,778$ trading days and $p = 92$ stocks ($p/n \approx 0.019$).

The Ridge regularization parameter is set to match the simulation, $\lambda/\gamma_n = 0.1$ with $\gamma_n = p/n$, giving $\lambda \approx 0.0019$, and trimming $\varepsilon = 0.1$. Critical values for the Ridge tests are the tabulated Gaussian-process quantiles. For the L_2^2 -CUSUM and L_∞ -CUSUM, whose null dis-

tributions depend on the unknown covariance Σ , critical values are obtained from 500 block-bootstrap replications with block length 20 (approximately one trading month), computed under the null by centering the observed data. For the Zhang–Lavitas tests, which are asymptotically pivotal by construction, critical values are obtained from 2,000 Monte Carlo replications of the statistic under $X_t \stackrel{\text{i.i.d.}}{\sim} N_p(0, I_p)$ with the same dimensions $(p, n) = (92, 4778)$; since the self-normalization ratio cancels the dependence on Σ , the identity covariance suffices.

6.1. *Results.* Table 6.1 summarizes the test results.

Method	Statistic	critical values ($\alpha = 0.05$)	Reject?
Ridge SC	9.459	2.976	Yes
Ridge MC	4.085	3.154	Yes
L_2^2 -CUSUM	0.228	0.617	No
L_∞ -CUSUM	0.229	0.311	No
Zhang–Lavitas SC	0.531	0.106	Yes
Zhang–Lavitas MC	0.296	0.103	Yes

TABLE 6.1

S&P 500 daily returns change-point test results ($p = 92$ stocks, $n = 4,778$ trading days, January 2007 to December 2025).

The Ridge SC test rejects decisively ($T_{\text{sc}} = 9.459$, more than three times the critical value 2.976), estimating the dominant change point at **March 5, 2009**—within four calendar days of the S&P 500 index’s famous trough on March 9, 2009, which marked the bottom of the Great Recession and the beginning of a prolonged bull market. The Ridge MC test also rejects ($T_{\text{mc}} = 4.085$ versus 3.154), with the argmax triple identifying an epidemic-type mean shift spanning approximately **May 2018 to March 2022**, a period that encompasses the COVID-19 crash (February–March 2020) and the subsequent recovery.

The Zhang–Lavitas tests, calibrated via their simulated pivotal null distribution, also reject both for the single and multiple change-point formulations. The Zhang–Lavitas SC statistic (0.531) exceeds its critical value (0.106) by a factor of five, locating the change point at March 6, 2009—essentially the same date as the Ridge SC estimate. The Zhang–Lavitas MC statistic (0.296 versus 0.103) identifies a boundary near November 24, 2008, during the acute phase of the financial crisis. These results confirm that the self-normalized approach, when properly calibrated, does detect the dominant crisis-era break.

By contrast, the L_2^2 -CUSUM and L_∞ -CUSUM fail to reject, with statistics (0.228 and 0.229) well below their bootstrap critical values (0.617 and 0.311). These unnormalized statistics are not pivotal and must rely on bootstrap calibration; without covariance normalization, they cannot effectively aggregate the coordinated but heterogeneous shift across all 92 series—sectors such as technology, energy, and utilities have very different return volatilities. The comparison between the two feasible pivotal methods (Ridge and Zhang–Lavitas) is also instructive: while both reject, the Ridge statistics exceed their critical values by substantially larger margins (3.18 for T_{sc} of Ridge versus 5.01 for Zhang–Lavitas SC), reflecting the greater signal amplification from ridge regularization relative to self-normalization. This margin matters for the recursive analysis below, where the Ridge test continues to detect finer structure that the Zhang–Lavitas test may miss.

6.2. *Recursive Change-Point Detection.* Having rejected the null with the Ridge MC test, we apply a recursive procedure to localize additional change points. The MC argmax triple (t_1, t_2, t_3) identifies both a change-point location at t_2 and an epidemic window $[t_1, t_3)$. At each step, if T_{mc} rejects, we split the segment into three parts—before, inside, and after the epidemic window—and recurse on each. Inside the epidemic, we further split at t_2 into two halves. Recursion terminates when the test does not reject or the segment contains fewer than 100 observations.

Table 6.2 reports the detected change points.

Depth	T_{mc}	n	Change point	Time window
0	4.085	4778	2020-04-17	[2018-05-23, 2022-03-09]
1	4.711	2867	2009-04-15	[2008-02-25, 2017-04-03]
1	4.638	478	2020-02-10	[2018-12-18, 2020-04-17]
1	5.384	478	2021-12-31	[2020-04-20, 2022-03-10]
2	5.016	287	2008-01-14	[2007-09-11, 2008-02-25]
2	4.497	287	2009-03-05	[2009-01-22, 2009-04-15]

TABLE 6.2

Recursive Ridge MC change-point detection on the S&P 500 panel. At each depth, the MC test is applied to the segment and, if it rejects, the argmax triple defines a three-way split. All tests use the same tabulated Gaussian-process critical value $cv_{0.05} = 3.154$.

After the recursion terminates, three segments show no further rejection: the pre-crisis segment (2007-01–2007-09, $T_{\text{mc}} = 0.14$), the long stable period 2009-04 to 2017-04 ($T_{\text{mc}} = 0.90$), and the post-COVID segment (2022-03–2025-12, $T_{\text{mc}} = 0.69$). The detected change points are economically interpretable:

- **January 14, 2008:** the onset of the subprime crisis, as write-downs at major banks accelerated and the S&P 500 entered a sustained decline.
- **March 5, 2009:** the market bottom—within four calendar days of the S&P 500 intraday low on March 9, 2009—after which the index began a prolonged recovery.
- **April 15, 2009:** the transition from crisis to post-crisis, with the epidemic window [2008-02, 2017-04] capturing the entire arc of the financial crisis and slow recovery under unconventional monetary policy.
- **February 10, 2020:** the eve of the COVID-19 crash; the S&P 500 peaked on February 19, 2020 and lost over 30% in the following month.
- **April 17, 2020:** the bottom of the COVID crash and the beginning of the rapid recovery, driven by unprecedented fiscal and monetary stimulus.
- **December 31, 2021:** the end of the post-COVID recovery regime, just before the Federal Reserve signaled aggressive rate hikes in January 2022, which triggered a broad market correction.

7. Discussion. In this paper, we developed a powerful and computationally tractable procedure for detecting multiple change points in the mean vectors of a sequence of independent observations. The proposed method is based on a ridge-type regularization of the classical CUSUM statistic. Using tools from random matrix theory, we derived the asymptotic null distribution under a high-dimensional regime in which the dimension is comparable to the sample size. The resulting test is self-normalized, leading to a pivotal limiting distribution that does not depend on unknown population parameters. Extensive simulation studies demonstrate that the proposed procedure achieves strong power across a wide range of alternatives and adapts well to different covariance structures.

An important direction for future research is the extension to dependent data, in particular to time series settings. When observations exhibit temporal dependence, it is natural to normalize the segment mean contrasts using an estimator of the long-run covariance matrix. The theoretical properties of high-dimensional sample autocovariance matrices have attracted considerable attention in recent years; see, for example, [Liu et al. \(2015\)](#). However, existing results often rely on restrictive assumptions on the dependence structure, which may limit their applicability in practice. More recently, [Deitmar \(2026\)](#) adopt a frequency-domain perspective and show that the spectrum of Daniell-smoothed periodograms satisfies asymptotic Marčenko–Pastur laws under mild conditions. These developments suggest a promising avenue for analyzing CUSUM-type statistics normalized by long-run covariance estimators based on smoothed periodograms. To pursue this direction, it is essential to establish a deterministic equivalent for the smoothed periodogram, analogous to part (iii) of Lemma 3.1. Deriving such results requires substantial additional technical development, and we leave this extension for future work.

Supplementary Material.

APPENDIX

Appendix A. Quantile Table.

REFERENCES

- Aston, J. A. and Kirch, C. (2018). High dimensional efficiency with applications to change point tests. *Electronic Journal of Statistics*, 12:1901–1947.
- Aue, A. and Horváth, L. (2013). Structural breaks in time series. *Journal of Time Series Analysis*, 34(1):1–16.
- Bai, Z. and Silverstein, J. W. (1998). No eigenvalues outside the support of the limiting spectral distribution of large-dimensional sample covariance matrices. *The Annals of Probability*, 26(1):316–345.
- Bai, Z. and Silverstein, J. W. (2004). CLT for linear spectral statistics of large-dimensional sample covariance matrices. *The Annals of Probability*, 32(1A):553–605.
- Bai, Z. and Silverstein, J. W. (2010). *Spectral Analysis of Large Dimensional Random Matrices*. Springer, New York, 2 edition.
- Billingsley, P. (2013). *Convergence of probability measures*. John Wiley & Sons.
- Chen, L. S., Paul, D., Prentice, R. L., and Wang, P. (2011). A regularized hotelling’s t^2 test for pathway analysis in proteomic studies. *Journal of the American Statistical Association*, 106(496):1345–1360.
- Cho, H. (2016). Change-point detection in panel data via double cusum statistic. *Electronic Journal of Statistics*, 10(2):2000–2038.
- Csörgő, M. and Horváth, L. (1997). *Limit Theorems in Change-Point Analysis*. Wiley Series in Probability and Statistics. John Wiley & Sons, Chichester.
- DeFriez, E. et al. (2016). Climate change-related regime shifts have altered spatial synchrony of ecological dynamics. *Global Change Biology*.
- Deitmar, B. (2026). Marchenko–pastur laws for daniell smoothed periodograms. *Journal of Time Series Analysis*.
- Enikeeva, F. and Harchaoui, Z. (2019). High-dimensional change-point detection under sparse alternatives. *The Annals of Statistics*, 47(4):2051–2079.
- Graham, N. A. et al. (2017). Recurrent patterns of dna copy number alterations in human tumors revealed by pan-cancer analysis. *Nature Communications*.
- Horváth, L. and Hušková, M. (2012). Change-point detection in panel data. *Journal of Time Series Analysis*, 33(4):631–648.
- Jiřák, M. (2012). On weak invariance principles for change-point statistics. *Journal of Multivariate Analysis*, 110:1–18.
- Jiřák, M. (2015). Uniform change point tests in high dimension. *The Annals of Statistics*, 43(6):2451–2483.
- Kirch, C., Muhsal, B., and Ombao, H. (2015). Detection of changes in multivariate time series with application to eeg data. *Journal of the American Statistical Association*, 110(511):1197–1216.
- Knowles, A. and Yin, J. (2017). Anisotropic local laws for random matrices. *Probability Theory and Related Fields*, 169(1):257–352.

TABLE 7.1

Simulated quantiles of the limiting null distribution of T_{sc} for different trimming parameters ε and grid sizes m . Each entry is based on $B = 200,000$ simulated Gaussian-process sample paths.

ε	$1 - \alpha$	$m = 1000$	$m = 2000$	$m = 4000$
.025	.90	2.853123	2.875801	2.896689
.025	.95	3.118827	3.142620	3.163149
.025	.99	3.642732	3.662845	3.678105
.050	.90	2.784101	2.805085	2.823106
.050	.95	3.059833	3.078606	3.097572
.050	.99	3.598786	3.613104	3.624232
.075	.90	2.733874	2.749903	2.767643
.075	.95	3.014937	3.029481	3.048557
.075	.99	3.560475	3.569917	3.581767
.100	.90	2.689027	2.703826	2.717823
.100	.95	2.974455	2.988155	3.003545
.100	.99	3.523465	3.529838	3.545666

TABLE 7.2

Simulated quantiles of the limiting null distribution of T_{mc} on the grid $\mathcal{G}(\varepsilon) = \{0, \varepsilon, 2\varepsilon, \dots, 1\}$. Let $\mathcal{D}_\varepsilon = \{(s, t, u) \in \mathcal{G}(\varepsilon)^3 : s < t < u, t - s \geq \varepsilon, u - t \geq \varepsilon\}$ denote the admissible triple set. Each entry is based on $B = 200,000$ simulated sample paths.

ε	$\#\mathcal{G}(\varepsilon)$	$\#\mathcal{D}_\varepsilon$	0.90	0.95	0.99
0.050	21	1330	3.403156	3.629294	4.073005
0.075	15	403	3.120785	3.356161	3.831476
0.100	11	165	2.941142	3.187065	3.676403

- Kringelbach, M. L. and Deco, G. (2020). Brain states and transitions: insights from computational neuroscience. *Cell Reports*.
- Li, H., Aue, A., and Paul, D. (2020a). High-dimensional general linear hypothesis tests via non-linear spectral shrinkage. *Bernoulli*, 26(4):2541–2571.
- Li, H., Aue, A., Paul, D., Peng, J., and Wang, P. (2020b). An adaptable generalization of Hotelling’s T^2 test in high dimension. *The Annals of Statistics*, 48(3):1815–1847.
- Liu, B., Zhou, C., Zhang, X., and Liu, Y. (2020). A unified data-adaptive framework for high dimensional change point detection. *Journal of the Royal Statistical Society Series B: Statistical Methodology*, 82(4):933–963.
- Liu, H., Aue, A., and Paul, D. (2015). On the marcenko-pastur law for linear time series. *ANNALS OF STATISTICS*, 43:2.
- Matteson, D. S. and James, N. A. (2014). A nonparametric approach for multiple change point analysis of multivariate data. *Journal of the American Statistical Association*, 109(505):334–345.
- Paul, D. and Aue, A. (2014). Random matrix theory in statistics: A review. *Journal of Statistical Planning and Inference*, 150:1–29.
- Shao, X. (2010). A self-normalized approach to confidence interval construction in time series. *Journal of the Royal Statistical Society Series B: Statistical Methodology*, 72(3):343–366.
- Shao, X. and Zhang, X. (2010). Testing for change points in time series. *Journal of the American Statistical Association*, 105(491):1228–1240.
- Wang, R., Zhu, C., Volgushev, S., and Shao, X. (2022). Inference for change points in high-dimensional data via selfnormalization. *The Annals of Statistics*, 50(2):781–806.
- Wang, T. and Samworth, R. J. (2018). High dimensional change point estimation via sparse projection. *Journal of the Royal Statistical Society: Series B*, 80(1):57–83.
- Yin, Y.-Q., Bai, Z.-D., and Krishnaiah, P. R. (1988). On the limit of the largest eigenvalue of the large dimensional sample covariance matrix. *Probability theory and related fields*, 78(4):509–521.
- Yu, Y. and Chen, X. (2021). High-dimensional change-point detection via graphical models. *Journal of the American Statistical Association*, 116(534):773–786.
- Zhang, N. R., Siegmund, D. O., Ji, H., and Li, J. Z. (2010). Detecting simultaneous change-points in multiple sequences. *Biometrika*, 97(3):631–645.

- Zhang, T. and Lavitas, L. (2018). Unsupervised self-normalized change-point testing for time series. *Journal of the American Statistical Association*, 113(522):637–648.
- Zhang, Y., Wang, R., and Shao, X. (2022). Adaptive inference for change points in high-dimensional data. *Journal of the American Statistical Association*, 117(540):1751–1762.

**SUPPLEMENTARY MATERIAL TO
“ADAPTABLE HIGH-DIMENSIONAL CHANGE POINT DETECTION VIA
RIDGE REGULARIZATION”**

BY HAORAN LI^{*1,a} AND HAOTIAN XU^{1,b}

¹Department of Mathematics and Statistics, Auburn University, ^ahzl0152@auburn.edu; ^bhaotian.xu@auburn.edu

S.1. Technical Lemmas. In this section, we collect several technical lemmas. Throughout, \mathcal{K} denotes a universal constant whose value may change from line to line, but which is independent of the parameter λ , the location t , the dimension p , and the sample size n . We use the notation $\|\cdot\|_2$ to denote the Euclidean norm of a vector or the spectral norm of a matrix, and $\|\cdot\|_\infty$ to denote the ℓ_∞ -norm of a vector or the uniform norm of a function. The notation A^T denotes either the transpose of a matrix A .

For a Hermitian matrix A with eigenvalues $\alpha_1 \geq \dots \geq \alpha_p$, we define its spectral distribution function by

$$F^A(\tau) = \frac{1}{p} \sum_{j=1}^p \mathbb{1}_{[\alpha_j, \infty)}(\tau).$$

LEMMA S.1.1 (Theorem A.43 of Bai and Silverstein (2010)). *Let A and B be two $p \times p$ Hermitian matrices. Then,*

$$\|F^A - F^B\|_\infty \leq \frac{1}{p} \text{rank}(A - B).$$

LEMMA S.1.2 (Woodbury Matrix Identity). *The following identity holds:*

$$(A + UCV)^{-1} = A^{-1} - A^{-1}U(C^{-1} + VA^{-1}U)^{-1}VA^{-1},$$

for matrices A, U, C, V of conformable sizes, assuming all inverses exist and are well-defined.

LEMMA S.1.3 (Burkholder). *Let $\{Y_i\}$ be a martingale difference sequence with respect to the increasing σ -field $\{\sigma_i\}$. Then, for $m \geq 2$*

$$\mathbb{E} \left| \sum_i Y_i \right|^m \leq \mathcal{K}_m \mathbb{E} \left(\sum_i \mathbb{E}(|Y_i|^2 | \sigma_{i-1}) \right)^{m/2} + \mathcal{K}_m \mathbb{E} \left(\sum_i |Y_i|^m \right).$$

Here, \mathcal{K}_m is a constant only depending on m .

LEMMA S.1.4 (Lemma 2.7 of Bai and Silverstein (1998)). *Let $W = (w_1, \dots, w_p)^T$, where w_i 's are i.i.d. real r.v.'s with mean 0 and variance 1. Let B be a deterministic (real or complex) matrix. Then, for any $j \geq 2$, we have*

$$\mathbb{E}|W^T B W - \text{tr}(B)|^m \leq \mathcal{K}_j (\mathbb{E} w_1^4 \text{tr}(B B^*))^{m/2} + \mathcal{K}_j \mathbb{E} w_1^{2m} \text{tr}[(B B^*)^{m/2}],$$

where \mathcal{K}_m is a constant only depending on m . Here B^ is the conjugate transpose of B .*

^{*}Corresponding author.

S.2. Proof of Theorem 3.1 and Theorem 3.2. First, under the null hypothesis $H_0 : \mu_j \equiv \mu$, the distribution of $D_\lambda(t_1, t_2, t_3)$ does not depend on μ , since the mean cancels out in both the pooled sample covariance matrix S_n and the segment mean difference $C_\lambda(t_1, t_2, t_3)$. Therefore, without loss of generality, we assume that $\mu = 0$.

We begin by working with the uncentered covariance matrix

$$\Omega_n = \frac{1}{n} \sum_{j=1}^n X_j X_j^T.$$

For any vectors u, v , and w in \mathbb{R}^n , define

$$G_\lambda(u, v, w) = p^{-1} u^T X^T (\Omega_n + \lambda I_p)^{-1} X v + p^{-1} \sum_{j=1}^n w_j^2 X_j^T (\Omega_n + \lambda I_p)^{-1} X_j.$$

Here, $X = (X_1, X_2, \dots, X_n)$ denotes the $p \times n$ data matrix.

In the subsequent analysis, we say that a vector $u \in \mathbb{R}^n$ is regular if we can find a universal constant \mathcal{K} , independent of n , such that

$$(S.1) \quad \|u\|_2 \leq \mathcal{K} \quad \text{and} \quad \sqrt{n} \|u\|_\infty \leq \mathcal{K}.$$

We have the following results.

THEOREM S.2.1. *Suppose that Conditions C1–C5 hold. Assume that the vectors u, v , and w are all regular in the sense of (S.1). Then, under the condition that $\mathbb{E}X_j = 0$,*

$$\frac{p^{1/2}}{\sqrt{\Gamma_n(\lambda)/2}} \frac{G_\lambda(u, v, w) - \mathbb{E}G_\lambda(u, v, w)}{\sqrt{\|u\|_2^2 \|v\|_2^2 + (u^T v)^2 + 2(w \cdot w)^T (w \cdot w) + 4(w \cdot u)^T (w \cdot v)}} \xrightarrow{D} N(0, 1).$$

Here, $(a \cdot b)$ is the Hadamard (element-wise) product of a and b . Namely, $(a \cdot b) = (a_1 b_1, a_2 b_2, \dots, a_n b_n)^T$.

THEOREM S.2.2. *Suppose that Conditions C1–C5. Then, if u, v and w are regular in the sense of (S.1) and $\mathbb{E}X_j = 0$,*

$$\sqrt{p} \left(\mathbb{E}G_\lambda(u, v, w) - (u^T v + w^T w) \Theta_n(\lambda) \right) \longrightarrow 0.$$

Before proceeding to the proof of Theorem S.2.1 and Theorem S.2.2, we describe a technique that will be frequently used in the following analysis. Fix $j \in \{1, \dots, n\}$. Then, Xu can be decomposed into two parts, one depending on X_j and the other independent of it, namely

$$Xu = u_j X_j + X_{(j)} u,$$

where $X_{(j)}$ denotes the matrix X with its j th column replaced by 0 and u_j is the j th entry of the vector u .

Using the Woodbury matrix identity (Lemma S.1.2), we can similarly decompose $(\Omega_n + \lambda I_p)^{-1}$ as

$$\begin{aligned} (\Omega_n + \lambda I_p)^{-1} &= (\Omega_n^{(j)} + \lambda I_p)^{-1} - \frac{n^{-1} (\Omega_n^{(j)} + \lambda I_p)^{-1} X_j X_j^T (\Omega_n^{(j)} + \lambda I_p)^{-1}}{1 + n^{-1} X_j^T (\Omega_n^{(j)} + \lambda I_p)^{-1} X_j} \\ &= R_j + \mathfrak{R}_j^\Omega, \quad \text{say.} \end{aligned}$$

Here,

$$\Omega_n^{(j)} = \frac{1}{n} \sum_{i \neq j} X_i X_i^T.$$

Notably, R_j is independent of X_j and \mathfrak{R}_j^Ω involves X_j .

Combining all these terms, we can decompose the quadratic term $u^T X^T (\Omega_n + \lambda I_p)^{-1} X v$ into two parts, one depending on X_j and the other independent of it, as

$$(S.2) \quad \begin{aligned} u^T X^T (\Omega_n + \lambda I_p)^{-1} X v &= u^T X_{(j)}^T R_j X_{(j)} v + \mathfrak{R}_j, \quad \text{with} \\ \mathfrak{R}_j &= v_j u^T X_{(j)}^T R_j X_j + u^T X_{(j)}^T \mathfrak{R}_j^\Omega X_{(j)} v + v_j u^T X_{(j)}^T \mathfrak{R}_j^\Omega X_j \\ &\quad + u_j X_j^T R_j X_{(j)} v + u_j v_j X_j^T R_j X_j + u_j X_j^T \mathfrak{R}_j^\Omega X_{(j)} v + u_j v_j X_j^T \mathfrak{R}_j^\Omega X_j. \end{aligned}$$

Similarly,

$$(S.3) \quad \begin{aligned} \sum_{i=1}^n w_i^2 X_i^T (\Omega_n + \lambda I_p)^{-1} X_i &= \sum_{i \neq j} w_i^2 X_i^T R_j X_i + \tilde{\mathfrak{R}}_j, \quad \text{with} \\ \tilde{\mathfrak{R}}_j &= \sum_{i \neq j} w_i^2 X_i^T \mathfrak{R}_j^\Omega X_i + w_j^2 X_j^T R_j X_j + w_j^2 X_j^T \mathfrak{R}_j^\Omega X_j. \end{aligned}$$

This decomposition is useful when applying a martingale difference sequence technique. In particular, denote the filtration generated by $\{X_j\}_{j \geq 1}$ to be $\{\mathcal{F}_j\}_{j \geq 1}$. Denote

$$\mathbb{E}_j = \mathbb{E}(\cdot \mid \mathcal{F}_j).$$

Then,

$$\begin{aligned} (\mathbb{E}_j - \mathbb{E}_{j-1}) \left[u^T X^T (\Omega_n + \lambda I_p)^{-1} X v + \sum_{i=1}^n w_i^2 X_i^T (\Omega_n + \lambda I_p)^{-1} X_i \right] \\ = (\mathbb{E}_j - \mathbb{E}_{j-1}) (\mathfrak{R}_j + \tilde{\mathfrak{R}}_j). \end{aligned}$$

PROOF OF THEOREM S.2.1 AND THEOREM S.2.2. Theorem S.2.1 and Theorem S.2.2 can be proved by closely following the arguments in Sections S.3 and S.9 of Li et al. (2020a). We therefore omit the details and only provide a brief overview of the proof. In particular, Li et al. (2020a) establishes Theorem S.2.1 and Theorem S.2.2 for the special case $w = 0$. The extension to general $w \neq 0$ proceeds analogously, with additional terms handled using similar arguments.

The main idea in the arguments in Li et al. (2020a) is to decompose $G_\lambda(u, v, 0)$ into a sum of martingale differences, after which the asymptotic normality of $G_\lambda(u, v, 0)$ follows from an application of a martingale central limit theorem. In particular, we can express $G_\lambda(u, v, 0) - \mathbb{E}G_\lambda(u, v, 0)$ as

$$G_\lambda(u, v, 0) - \mathbb{E}G_\lambda(u, v, 0) = \sum_{j=1}^n (\mathbb{E}_j - \mathbb{E}_{j-1}) G_\lambda(u, v, 0).$$

The key arguments in Li et al. (2020a) are to control the fluctuation of

$$(\mathbb{E}_j - \mathbb{E}_{j-1}) G_\lambda(u, v, 0).$$

To this end, with the decomposition shown in (S.2), we have

$$(\mathbb{E}_j - \mathbb{E}_{j-1}) G_\lambda(u, v, 0) = p^{-1} (\mathbb{E}_j - \mathbb{E}_{j-1}) \mathfrak{R}_j.$$

The key steps are then to construct concentration bounds of the martingale difference sequence $p^{-1/2} (\mathbb{E}_j - \mathbb{E}_{j-1}) \mathfrak{R}_j$, using concentration inequalities for quadratic forms, in particular Lemma S.1.4. The details are presented in Section S.3.1 of Li et al. (2020a).

Secondly, to deal with the expectation,

$$\begin{aligned}\mathbb{E}G_\lambda(u, v, 0) &= \left(\sum_{j=1}^n u_j v_j \right) p^{-1} \mathbb{E} X_1^T (\Omega_n + \lambda I_p)^{-1} X_1 \\ &\quad + \left(\sum_{i \neq j} u_i v_j \right) p^{-1} \mathbb{E} X_1^T (\Omega_n + \lambda I_p)^{-1} X_2.\end{aligned}$$

It is shown in Section S.3.3 of Li et al. (2020a) that

$$\begin{aligned}p^{-1} \mathbb{E} X_1^T (\Omega_n + \lambda I_p)^{-1} X_1 &= \Theta_n(\lambda) + o(p^{-1/2}), \\ p^{-1} \mathbb{E} X_1^T (\Omega_n + \lambda I_p)^{-1} X_2 &= o(p^{-1/2}),\end{aligned}$$

It completes the proof of Theorem S.2.1 and Theorem S.2.2 when $w = 0$.

It is worth mentioning that Li et al. (2020a) adopts a variable truncation technique in the proof. See Equation (A.4) of Li et al. (2020a) for details. This technique is proposed in Yin et al. (1988) and has been used in cornerstone works in RMT such as Bai and Silverstein (2004). Arguments in Section S.3.1 of Li et al. (2020a) work under truncated random variables. The results are extended to Condition C1 in Li et al. (2020a).

When $w \neq 0$, we only need to make the following modification. First, with the decomposition in (S.2) and (S.3),

$$\begin{aligned}G_\lambda(u, v, w) &= p^{-1} \left(u^T X_{(j)}^T R_j X_{(j)} v + \sum_{i \neq j} w_i^2 X_i^T R_j X_i \right) \\ &\quad + p^{-1} \mathfrak{R}_j + p^{-1} \tilde{\mathfrak{R}}_j.\end{aligned}$$

Then,

$$(\mathbb{E}_j - \mathbb{E}_{j-1}) G_\lambda(u, v, w) = p^{-1} (\mathbb{E}_j - \mathbb{E}_{j-1}) (\mathfrak{R}_j + \tilde{\mathfrak{R}}_j).$$

Note that the terms in $\tilde{\mathfrak{R}}_j$ has the same structure as those in \mathfrak{R}_j . Indeed, the terms in $\tilde{\mathfrak{R}}_j$ can be absorbed into those in \mathfrak{R}_j . For example, the first term in $\tilde{\mathfrak{R}}_j$ can be absorbed into the second term in \mathfrak{R}_j as

$$u^T X_{(j)}^T \mathfrak{R}_j^\Omega X_{(j)} v + \sum_{i \neq j} w_i^2 X_i^T \mathfrak{R}_j^\Omega X_i = \sum_{i \neq j} (u_i v_i + w_i^2) X_i^T \mathfrak{R}_j^\Omega X_i + \sum_{i, k \neq j, i \neq k} u_i v_k X_i^T \mathfrak{R}_j^\Omega X_k.$$

Therefore, we can treat the sum $\mathfrak{R}_j + \tilde{\mathfrak{R}}_j$ in the same manner. Theorem S.2.1 is then established by deriving concentration bounds for the martingale difference sequence $(\mathbb{E}_j - \mathbb{E}_{j-1}) (\mathfrak{R}_j + \tilde{\mathfrak{R}}_j)$. The arguments closely follow those in Section S.3 of Li et al. (2020a). We therefore omit the details.

The convergence of the expectation

$$\begin{aligned}\mathbb{E}G_\lambda(u, v, w) &= \left(\sum_{j=1}^n u_j v_j + w_j^2 \right) p^{-1} \mathbb{E} X_1^T (\Omega_n + \lambda I_p)^{-1} X_1 \\ &\quad + \left(\sum_{i \neq j} u_i v_j \right) p^{-1} \mathbb{E} X_1^T (\Omega_n + \lambda I_p)^{-1} X_2.\end{aligned}$$

follows directly from the convergence of $p^{-1} \mathbb{E} X_1^T (\Omega_n + \lambda I_p)^{-1} X_1$ and $p^{-1} \mathbb{E} X_1^T (\Omega_n + \lambda I_p)^{-1} X_2$. \square

Next, we show an increment bound on $\sqrt{p}(G_\lambda(u, v, w) - \mathbb{E}G_\lambda(u, v, w))$ when the vectors u, v and w are shifted.

THEOREM S.2.3. *Suppose that Conditions C1–C5 hold. Assume that $u_1, v_1, w_1, u_2, v_2,$ and w_2 are all regular in the sense of (S.1), and $\mathbb{E}X_j = 0$. Then, we can find a universal constant \mathcal{K} such that*

$$\begin{aligned} & \mathbb{E} \left| \sqrt{p} \left(G_\lambda(u_1, v_1, w_1) - \mathbb{E}G_\lambda(u_1, v_1, w_1) \right) - \sqrt{p} \left(G_\lambda(u_2, v_2, w_2) - \mathbb{E}G_\lambda(u_2, v_2, w_2) \right) \right|^2 \\ & \leq \mathcal{K} \left(\|u_1 - u_2\|_2^2 + \|v_1 - v_2\|_2^2 + \|w_1 - w_2\|_2^2 \right). \end{aligned}$$

PROOF OF THEOREM S.2.3. We begin by bounding the increment

$$\begin{aligned} & \left(G_\lambda(u_1, v, w) - \mathbb{E}G_\lambda(u_1, v, w) \right) - \left(G_\lambda(u_2, v, w) - \mathbb{E}G_\lambda(u_2, v, w) \right) \\ & = G_\lambda(u_1 - u_2, v, w) - \mathbb{E}G_\lambda(u_1 - u_2, v, w), \end{aligned}$$

for any regular vectors $u_1, u_2, v,$ and w satisfying (S.1).

Using a martingale decomposition technique,

$$\mathbb{E} \left| G_\lambda(u_1 - u_2, v, w) - \mathbb{E}G_\lambda(u_1 - u_2, v, w) \right|^2 = \sum_{j=1}^n \mathbb{E} \left| (\mathbb{E}_j - \mathbb{E}_{j-1}) G_\lambda(u_1 - u_2, v, w) \right|^2.$$

With the decomposition of $G_\lambda(u, v, w)$ shown in (S.2), we have

$$\begin{aligned} & (\mathbb{E}_j - \mathbb{E}_{j-1}) G_\lambda(u_1 - u_2, v, w) \\ & = p^{-1} (\mathbb{E}_j - \mathbb{E}_{j-1}) \left(v_j (u_1 - u_2)^T X_{(j)}^T R_j X_j + (u_{1j} - u_{2j}) X_j^T R_j X_{(j)} v \right. \\ \text{(S.4)} \quad & + (u_{1j} - u_{2j}) v_j X_j^T R_j X_j + (u_{1j} - u_{2j}) v_j X_j^T \mathfrak{R}_j^\Omega X_j + v_j (u_1 - u_2)^T X_{(j)}^T \mathfrak{R}_j^\Omega X_j \\ & \left. + (u_{1j} - u_{2j}) v^T X_{(j)}^T \mathfrak{R}_j^\Omega X_j + (u_1 - u_2)^T X_{(j)}^T \mathfrak{R}_j^\Omega X_{(j)} v \right). \end{aligned}$$

Then, it suffices to derive concentration bounds for the variance of all terms on the right-hand side of the decomposition.

We summarize the key arguments in the following lemma, which directly follows from the application of Lemmas S.1.3 and S.1.4.

LEMMA S.2.1. *Suppose that Conditions C1–C5 hold. Assume that v satisfies Condition (S.1), and $\mathbb{E}X_j = 0$. Then,*

$$\mathbb{E} | p^{-1} X_j^T R_j X_j - p^{-1} \text{tr}(R_j) |^m = O(p^{-m/2}), \quad m \geq 2.$$

Secondly, for $m = 2, 4,$

$$\begin{aligned} \mathbb{E} | p^{-1} X_j^T R_j X_{(j)} v |^m & \leq \mathcal{K} p^{-m} \mathbb{E} | v^T X_{(j)}^T R_j^2 X_{(j)} v |^{m/2} \\ & \leq \mathcal{K} (1/\lambda^m) p^{-m} \|v\|_2^m [\text{tr}(\Sigma)]^{m/2} = O(\|v\|_2^m p^{-m/2}). \end{aligned}$$

The bounds are uniform in j . Here, we are using the fact that the spectral norm $\|R_j\|_2 \leq 1/\lambda$.

Using Lemma S.2.1 and Jensen's inequality, the first term in the decomposition (S.4) is such that

$$\begin{aligned} p^{-1} \sum_{j=1}^n \mathbb{E} | (\mathbb{E}_j - \mathbb{E}_{j-1}) v_j^2 (u_1 - u_2)^T X_{(j)}^T R_j X_j |^2 & \leq p^{-1} \sum_{j=1}^n v_j^2 \mathbb{E} | (u_1 - u_2)^T X_{(j)}^T R_j X_j |^2 \\ & \leq \mathcal{K} \|u_1 - u_2\|_2^2 \sum_{j=1}^n \|v\|_\infty^2 \leq \mathcal{K} \|u_1 - u_2\|_2^2. \end{aligned}$$

Similarly, the second term in the decomposition is such that

$$\begin{aligned} & p^{-1} \sum_{j=1}^n \mathbb{E} \left| (\mathbb{E}_j - \mathbb{E}_{j-1})(u_{1j} - u_{2j}) X_j^T R_j X_{(j)} v \right|^2 \\ & \leq p^{-1} \sum_{j=1}^n (u_{1j} - u_{2j})^2 \mathbb{E} |X_j^T R_j X_{(j)} v|^2 \leq \mathcal{K} \|u_1 - u_2\|_2^2 \|v\|_2^2. \end{aligned}$$

The third term in the decomposition is such that

$$\begin{aligned} & p^{-1} \sum_{j=1}^n \mathbb{E} |(\mathbb{E}_j - \mathbb{E}_{j-1})(u_{1j} - u_{2j}) v_j X_j^T R_j X_j|^2 \\ & \leq p^{-1} \sum_{j=1}^n (u_{1j} - u_{2j})^2 v_j^2 \mathbb{E} |X_j^T R_j X_j - \text{tr} R_j|^2 \leq \mathcal{K} \|u_1 - u_2\|_2^2. \end{aligned}$$

The fourth term in the decomposition is such that

$$\begin{aligned} & p^{-1} \sum_{j=1}^n \mathbb{E} |(\mathbb{E}_j - \mathbb{E}_{j-1})(u_{1j} - u_{2j}) v_j X_j^T \mathfrak{R}_j^\Omega X_j|^2 \\ & = p^{-1} \sum_{j=1}^n (u_{1j} - u_{2j})^2 v_j^2 \mathbb{E} \left| (\mathbb{E}_j - \mathbb{E}_{j-1}) \frac{n^{-1} (X_j^T R_j X_j)^2}{1 + n^{-1} X_j^T R_j X_j} \right|^2 \\ & \leq \mathcal{K} \sum_{j=1}^n (u_{1j} - u_{2j})^2 \mathbb{E} \left| (\mathbb{E}_j - \mathbb{E}_{j-1}) \frac{(n^{-1} X_j^T R_j X_j)^2}{1 + n^{-1} X_j^T R_j X_j} \right|^2 \\ & \leq \mathcal{K} \sum_{j=1}^n (u_{1j} - u_{2j})^2 \mathbb{E} \left| (\mathbb{E}_j - \mathbb{E}_{j-1}) n^{-1} X_j^T R_j X_j + (\mathbb{E}_j - \mathbb{E}_{j-1}) \frac{1}{1 + n^{-1} X_j^T R_j X_j} \right|^2 \\ & \leq \mathcal{K} \sum_{j=1}^n (u_{1j} - u_{2j})^2 \mathbb{E} \left| (\mathbb{E}_j - \mathbb{E}_{j-1}) n^{-1} X_j^T R_j X_j \right|^2 \\ & \quad + \mathcal{K} \sum_{j=1}^n (u_{1j} - u_{2j})^2 \mathbb{E} \left| (\mathbb{E}_j - \mathbb{E}_{j-1}) \frac{1}{1 + n^{-1} X_j^T R_j X_j} \right|^2 \\ & \leq \mathcal{K} \|u_1 - u_2\|_2^2 \mathbb{E} \left| n^{-1} X_1^T R_1 X_1 - n^{-1} \text{tr} R_1 \right|^2 \\ & \quad + \mathcal{K} \|u_1 - u_2\|_2^2 \mathbb{E} \left| \frac{n^{-1} X_1^T R_1 X_1 - n^{-1} \text{tr}(R_1)}{(1 + n^{-1} X_1^T R_1 X_1)(1 + n^{-1} \text{tr}(R_1))} \right|^2 \\ & \leq \mathcal{K} \|u_1 - u_2\|_2^2 \mathbb{E} \left| n^{-1} X_j^T R_j X_j - n^{-1} \text{tr} R_j \right|^2 \leq \mathcal{K} \|u_1 - u_2\|_2^2. \end{aligned}$$

The fifth term in the decomposition is such that

$$\begin{aligned} & p^{-1} \sum_{j=1}^n \mathbb{E} |(\mathbb{E}_j - \mathbb{E}_{j-1}) v_j (u_1 - u_2)^T X_{(j)}^T \mathfrak{R}_j^\Omega X_j|^2 \\ & = p^{-1} \sum_{j=1}^n v_j^2 \mathbb{E} \left| (\mathbb{E}_j - \mathbb{E}_{j-1}) \frac{n^{-1} X_j^T R_j X_j}{1 + n^{-1} X_j^T R_j X_j} X_j^T R_j X_{(j)} (u_1 - u_2) \right|^2 \end{aligned}$$

$$\begin{aligned}
&\leq \mathcal{K} p^{-1} \sum_{j=1}^n v_j^2 \mathbb{E} \left| X_j^T R_j X_{(j)} (u_1 - u_2) \right|^2 \\
&\leq \mathcal{K} p^{-1} \sum_{j=1}^n v_j^2 p \|u_1 - u_2\|_2^2 \leq \mathcal{K} \|u_1 - u_2\|_2^2.
\end{aligned}$$

The sixth term is treated in a similar manner as the fifth term, and we obtain

$$p^{-1} \sum_{j=1}^n \mathbb{E} |(\mathbb{E}_j - \mathbb{E}_{j-1})(u_{1j} - u_{2j}) v^T X_{(j)}^T \mathfrak{R}_j^\Omega X_j|^2 \leq \mathcal{K} \|u_1 - u_2\|_2^2.$$

The last term in the decomposition (S.4) requires slightly more delicate treatment. Call $\mathcal{H}_j = R_j X_{(j)} v (u_1 - u_2)^T X_{(j)}^T R_j$. Then

$$\begin{aligned}
p^{-2} \mathbb{E} \operatorname{tr}(\mathcal{H}_j \mathcal{H}_j^T) &= p^{-2} \mathbb{E} \left(v^T X_{(j)}^T R_j^2 X_{(j)} v \right) \left((u_1 - u_2)^T X_{(j)}^T R_j^2 X_{(j)} (u_1 - u_2) \right) \\
&\leq \mathcal{K} \|v\|_2^2 \|u_1 - u_2\|_2^2.
\end{aligned}$$

Notice that

$$\begin{aligned}
&(\mathbb{E}_j - \mathbb{E}_{j-1})(u_1 - u_2)^T X_{(j)}^T \mathfrak{R}_j^\Omega X_{(j)} v \\
&= (\mathbb{E}_j - \mathbb{E}_{j-1}) \left(\frac{n^{-1} X_j^T \mathcal{H}_j X_j}{1 + n^{-1} X_j^T R_j X_j} - \frac{n^{-1} \operatorname{tr}(\mathcal{H}_j)}{1 + n^{-1} \operatorname{tr}(R_j)} \right) \\
&= (\mathbb{E}_j - \mathbb{E}_{j-1}) \left(\frac{n^{-1} X_j^T \mathcal{H}_j X_j - n^{-1} \operatorname{tr}(\mathcal{H}_j)}{1 + n^{-1} X_j^T R_j X_j} \right) \\
&\quad - (\mathbb{E}_j - \mathbb{E}_{j-1}) n^{-1} \operatorname{tr}(\mathcal{H}_j) \left[\frac{1}{1 + n^{-1} \operatorname{tr}(R_j)} - \frac{1}{1 + n^{-1} X_j^T R_j X_j} \right].
\end{aligned}$$

Using Lemma S.1.4,

$$\begin{aligned}
\mathbb{E} \left| \frac{n^{-1} X_j^T \mathcal{H}_j X_j - n^{-1} \operatorname{tr}(\mathcal{H}_j)}{1 + n^{-1} X_j^T R_j X_j} \right|^2 &\leq \mathbb{E} |n^{-1} X_j^T \mathcal{H}_j X_j - n^{-1} \operatorname{tr}(\mathcal{H}_j)|^2 \\
&\leq \mathcal{K} n^{-2} \mathbb{E} \operatorname{tr}[\mathcal{H}_j \mathcal{H}_j^T] \leq \mathcal{K} \|v\|_2^2 \|u_1 - u_2\|_2^2.
\end{aligned}$$

Moreover,

$$\begin{aligned}
\mathbb{E} \left| n^{-1} \operatorname{tr}(\mathcal{H}_j) \left(\frac{1}{1 + n^{-1} \operatorname{tr}(R_j)} - \frac{1}{1 + n^{-1} X_j^T R_j X_j} \right) \right|^2 &\leq 4 \mathbb{E} |n^{-1} \operatorname{tr}(\mathcal{H}_j)|^2 \\
&\leq \mathcal{K} \|v\|_2^2 \|u_1 - u_2\|_2^2.
\end{aligned}$$

In summary, we obtain that

$$\mathbb{E} p \left| G_\lambda(u_1 - u_2, v, w) - \mathbb{E} G_\lambda(u_1 - u_2, v, w) \right|^2 \leq \mathcal{K} \|u_1 - u_2\|_2^2.$$

On the other hand, due to very similar arguments, we can show that

$$\mathbb{E} p \left| \left(G_\lambda(u, v, w_1) - \mathbb{E} G_\lambda(u, v, w_1) \right) - \left(G_\lambda(u, v, w_2) - \mathbb{E} G_\lambda(u, v, w_2) \right) \right|^2 \leq \mathcal{K} \|w_1 - w_2\|_2^2,$$

for any regular vectors u and v satisfying (S.1).

Note that

$$\begin{aligned} & G(u_1, v_1, w_1) - G(u_2, v_2, w_2) \\ &= G(u_1 - u_2, v_1, w_1) + G(u_2, v_1 - v_2, w_1) + G(u_2, v_2, w_1 - w_2). \end{aligned}$$

The statement of Theorem S.2.3 now follows from the triangle inequality. \square

Next, recall the definition of the scanning set $\mathcal{T}(\varepsilon)$ as in (2.8). Take any element $(t_1, t_2, t_3) \in \mathcal{T}(\varepsilon)$ and define

$$(S.5) \quad \tilde{u}_n(t_1, t_2, t_3) = \sqrt{n} \left(\underbrace{0, \dots, 0}_{k(t_1)-1}, \underbrace{\frac{-1}{k(t_2) - k(t_1)}, \dots, \frac{-1}{k(t_2) - k(t_1)}}_{k(t_2)-k(t_1)}, \underbrace{\frac{1}{k(t_3) - k(t_2)}, \dots, \frac{1}{k(t_3) - k(t_2)}}_{k(t_2)-k(t_1)}, \underbrace{0, \dots, 0}_{n-k(t_3)+1} \right)^T,$$

Then, $n^{-1/2} X \tilde{u}_n(t_1, t_2, t_3)$ is the difference between the segment means on $[t_1, t_2)$ and $[t_2, t_3)$. Since $\varepsilon > 0$, it is straightforward that, for any $(t_1, t_2, t_3) \in \mathcal{T}(\varepsilon)$, $\tilde{u}_n(t_1, t_2, t_3)$ is regular in the sense of (S.1).

Recall the definition of $u(x; t_1, t_2, t_3)$ and the inner product function

$$\kappa(t_1, t_2, t_3; m_1, m_2, m_3) = \int_0^1 u(x; t_1, t_2, t_3) u(x; m_1, m_2, m_3) dx.$$

as in (3.4) and (3.5). It is straightforward to show that

$$(S.6) \quad (\tilde{u}_n(t_1, t_2, t_3))^T \tilde{u}_n(m_1, m_2, m_3) = \kappa(t_1, t_2, t_3; m_1, m_2, m_3) + o(p^{-1/2}).$$

In particular,

$$\|\tilde{u}_n(t_1, t_2, t_3)\|_2^2 = \frac{n}{N(t_1, t_2, t_3)} = \kappa(t_1, t_2, t_3) + o(p^{-1/2}).$$

Construct the following stochastic process on $(\mathcal{T}(\varepsilon))^2$:

$$\begin{aligned} & \mathcal{G}_\lambda(t_1, t_2, t_3; m_1, m_2, m_3) \\ &= \frac{p^{1/2}}{\sqrt{\Gamma_n(\lambda)/2}} \left[p^{-1} (\tilde{u}_n(t_1, t_2, t_3))^T X^T (\Omega_n + \lambda I_p)^{-1} X \tilde{u}_n(m_1, m_2, m_3) \right. \\ & \quad \left. - (\tilde{u}_n(t_1, t_2, t_3))^T \tilde{u}_n(m_1, m_2, m_3) \Theta_n(\lambda) \right]. \end{aligned}$$

Then $\mathcal{G}_\lambda(t_1, t_2, t_3; t_1, t_2, t_3)$ corresponds to the standardized statistic $D_\lambda(t_1, t_2, t_3)$ when the normalization is performed using the deterministic quantities $\Theta_n(\lambda)$ and $\Gamma_n(\lambda)$ in place of their estimators $\hat{\Theta}(\lambda)$ and $\hat{\Gamma}(\lambda)$. Here, we also allow that (t_1, t_2, t_3) and (m_1, m_2, m_3) differ.

We shall show the weak convergence of the process $\mathcal{G}_\lambda(t_1, t_2, t_3; m_1, m_2, m_3)$. Let

$$\mathcal{G}_\lambda^\infty(t_1, t_2, t_3; m_1, m_2, m_3), \quad (t_1, t_2, t_3) \text{ and } (m_1, m_2, m_3) \in \mathcal{T}(\varepsilon)$$

be a centered Gaussian process on $(\mathcal{T}(\varepsilon))^2$ with the covariance kernel

$$\begin{aligned} & \mathbb{E}\mathcal{G}_\lambda^\infty(t_1, t_2, t_3; m_1, m_2, m_3)\mathcal{G}_\lambda^\infty(t'_1, t'_2, t'_3; m'_1, m'_2, m'_3) \\ &= \kappa(t_1, t_2, t_3; t'_1, t'_2, t'_3)\kappa(m_1, m_2, m_3; m'_1, m'_2, m'_3) \\ & \quad + \kappa(t_1, t_2, t_3; m'_1, m'_2, m'_3)\kappa(m_1, m_2, m_3; t'_1, t'_2, t'_3). \end{aligned}$$

By the Kolmogorov continuity theorem, the process is well-defined, and its sample path is a.s. continuous.

THEOREM S.2.4. *Suppose that Conditions **C1–C5** hold. Assume that $\mathbb{E}X_j = 0$. Then, the process*

$$\mathcal{G}_\lambda(t_1, t_2, t_3; m_1, m_2, m_3), \quad \text{on } (\mathcal{T}(\varepsilon))^2,$$

converges weakly, with respect to the Skorohod J_1 -topology, to

$$\mathcal{G}_\lambda^\infty(t_1, t_2, t_3; m_1, m_2, m_3), \quad \text{on } (\mathcal{T}(\varepsilon))^2.$$

PROOF OF THEOREM S.2.4. We use Theorem 12.3 of Billingsley (2013). In particular, we only need to show (i) the finite-dimensional convergence and (ii) the tightness of $\mathcal{G}_\lambda(t_1, t_2, t_3; m_1, m_2, m_3)$.

First, the finite-dimensional convergence follows directly from Theorem S.2.1. Indeed, take any finite group of indices

$$\left(t_1^{(j)}, t_2^{(j)}, t_3^{(j)}; m_1^{(j)}, m_2^{(j)}, m_3^{(j)}\right), \quad j = 1, \dots, J.$$

Any fixed linear combination of the values of \mathcal{G}_λ at these indices takes the form of a generic quadratic form $G_\lambda(u, v, w)$ for some regular vectors u, v, w . Then, Theorem S.2.1 guarantees the asymptotic normality of the linear combination. Here, we also need the convergence of the inner products of the form $(\tilde{u}_n(t_1, t_2, t_3))^T \tilde{u}_n(m_1, m_2, m_3)$ given in (S.6).

Second, the tightness of $\mathcal{G}_\lambda(t_1, t_2, t_3; m_1, m_2, m_3)$ is implied by

- (1) the tightness of $\mathcal{G}_\lambda(t_1, t_2, t_3; m_1, m_2, m_3)$ at a fixed value $(t_1, t_2, t_3; m_1, m_2, m_3)$;
- (2) a moment bound on the increment in the sense:

For any $(t_1, t_2, t_3; m_1, m_2, m_3), (t'_1, t'_2, t'_3; m'_1, m'_2, m'_3)$ in $(\mathcal{T}(\varepsilon))^2$, we have

$$\begin{aligned} & \mathbb{E}\left|\mathcal{G}_\lambda(t_1, t_2, t_3; m_1, m_2, m_3) - \mathcal{G}_\lambda(t'_1, t'_2, t'_3; m'_1, m'_2, m'_3)\right|^2 \\ & \leq \mathcal{K}\|(t_1, t_2, t_3) - (t'_1, t'_2, t'_3)\|_1 + \mathcal{K}\|(m_1, m_2, m_3) - (m'_1, m'_2, m'_3)\|_1. \end{aligned}$$

Result (1) directly follows the finite-dimensional convergence. Result (2) follows from the combination of Theorem S.2.3, Theorem S.2.2, and the fact that

$$\|\tilde{u}_n(t_1, t_2, t_3) - \tilde{u}_n(t'_1, t'_2, t'_3)\|_2^2 \leq \mathcal{K}\|(t_1, t_2, t_3) - (t'_1, t'_2, t'_3)\|_1.$$

□

While the previous analysis focuses on the uncentered sample covariance matrix Ω_n , we now proceed to the analysis of the CUSUM defined with the centered sample covariance matrix

$$S_n = \frac{1}{n} \sum_{j=1}^n (X_j - \bar{X})(X_j - \bar{X})^T.$$

For any u and v , using the Woodbury matrix identity (Lemma S.1.2),

$$\begin{aligned} & u^T X^T (S_n + \lambda I_p)^{-1} X v \\ &= u^T X^T [\Omega_n + \lambda I_p - \bar{X} \bar{X}^T]^{-1} X v \\ &= u^T X^T (\Omega_n + \lambda I_p)^{-1} X v + \frac{u^T X^T (\Omega_n + \lambda I_p)^{-1} \bar{X} \bar{X}^T (\Omega_n + \lambda I_p)^{-1} X v}{1 - \bar{X}^T (\Omega_n + \lambda I_p)^{-1} \bar{X}}. \end{aligned}$$

Here, we need to verify that $\bar{X}^T (\Omega_n + \lambda I_p)^{-1} \bar{X}$ is bounded away from 1 with high probability, so that the denominator in the preceding display is well defined with high probability. To this end, let

$$a_n = \sqrt{p} (1/n, 1/n, \dots, 1/n)^T.$$

Then

$$G_\lambda(a_n, a_n, 0) = \bar{X}^T (\Omega_n + \lambda I_p)^{-1} \bar{X}.$$

It is straightforward that a_n is regular. By Theorem S.2.1,

$$G_\lambda(a_n, a_n, 0) - (a_n^T a_n) \Theta_n(\lambda) = G_\lambda(a_n, a_n, 0) - \gamma_n \Theta_n(\lambda) = o_p(1).$$

Therefore, it suffices to show that

$$1 - \gamma_n \Theta_n(\lambda) = 1 - \gamma_n + \gamma_n \lambda \varphi_n(-\lambda)$$

is bounded away from 0 for any $\lambda > 0$. This follows directly from Section S.2 of Li et al. (2020a). In particular, they show that for any closed and bounded subset $\mathcal{S} \subset \mathbb{C} \setminus \mathbb{R}^+$,

$$\inf_{z \in \mathcal{S}} |1 - \gamma_n - \gamma_n z \varphi_n(z)| > 0.$$

Consequently, there exists a constant $\mathcal{K} > 0$ such that

$$\mathbb{P}(|1 - \bar{X}^T (\Omega_n + \lambda I_p)^{-1} \bar{X}| > \mathcal{K}) \rightarrow 1,$$

for any $\lambda > 0$.

The analysis implies that

$$\begin{aligned} & p^{-1} u^T X^T (S_n + \lambda I_p)^{-1} X v \\ &= G_\lambda(u, v, 0) + G_\lambda(a, u, 0) G_\lambda(a, v, 0) [1 - G_\lambda(a, a, 0)]^{-1}, \end{aligned}$$

with $[1 - G_\lambda(a, a, 0)]^{-1}$ bounded away from singularity with high probability.

With the definition of $\tilde{u}_n(t_1, t_2, t_3)$ and $\mathcal{G}_\lambda(t_1, t_2, t_3; m_1, m_2, m_3)$, the statistic

$$p^{-1} V_\lambda(t_1, t_2, t_3) = N(t_1, t_2, t_3) n^{-1} p^{-1} (\tilde{u}_n(t_1, t_2, t_3))^T X^T (S_n + \lambda I_p)^{-1} X \tilde{u}_n(t_1, t_2, t_3)$$

is $\mathcal{G}_\lambda(t_1, t_2, t_3; t_1, t_2, t_3)$ after the scaling of $N(t_1, t_2, t_3)/n$. Applying the functional delta method, the asymptotic Gaussianity of the process

$$\sqrt{p} \frac{p^{-1} V_\lambda(t_1, t_2, t_3) - \Theta_n(\lambda)}{\sqrt{\Gamma_n(\lambda)/2}}, \quad (t_1, t_2, t_3) \in \mathcal{T}(\varepsilon),$$

follows from the asymptotic Gaussianity of the process $\mathcal{G}_\lambda(t_1, t_2, t_3; m_1, m_2, m_3)$ established in Theorem S.2.4.

Recall the uniform consistency of $\hat{\Theta}(\lambda)$ and $\hat{\Gamma}(\lambda)$ established in Lemma 3.1. It follows that the empirically standardized statistic

$$D_\lambda(t_1, t_2, t_3) = \sqrt{p} \frac{p^{-1} V_\lambda(t_1, t_2, t_3) - \hat{\Theta}(\lambda)}{\sqrt{\hat{\Gamma}(\lambda)}}, \quad (t_1, t_2, t_3) \in \mathcal{T}(\varepsilon),$$

converges weakly, with respect to the Skorohod J_1 topology, to the Gaussian process $G(t_1, t_2, t_3)$ on $\mathcal{T}(\varepsilon)$. That is,

$$\{D_\lambda(t_1, t_2, t_3), (t_1, t_2, t_3) \in \mathcal{T}(\varepsilon)\} \rightsquigarrow \{G(t_1, t_2, t_3), (t_1, t_2, t_3) \in \mathcal{T}(\varepsilon)\}.$$

Lastly, by the Kolmogorov continuity theorem, the sample paths of $\{G(t_1, t_2, t_3)\}$ are almost surely continuous. Therefore, by the continuous mapping theorem,

$$T_{\text{sc}}(\varepsilon, \lambda) = \max_{t \in [\varepsilon, 1-\varepsilon]} D_\lambda(0, t, 1) \xrightarrow{D} \sup_{t \in [\varepsilon, 1-\varepsilon]} G(0, t, 1),$$

$$T_{\text{mc}}(\varepsilon, \lambda) = \max_{(t_1, t_2, t_3) \in \mathcal{T}(\varepsilon)} D_\lambda(t_1, t_2, t_3) \xrightarrow{D} \sup_{(t_1, t_2, t_3) \in \mathcal{T}(\varepsilon)} G(t_1, t_2, t_3),$$

$$T_{\text{mc}}^*(\varepsilon, \lambda) = \max_{(t_1, t_2, t_3) \in \mathcal{T}_*(\varepsilon)} D_\lambda(t_1, t_2, t_3) \xrightarrow{D} \sup_{(t_1, t_2, t_3) \in \mathcal{T}_*(\varepsilon)} G(t_1, t_2, t_3).$$

This completes the proof of Theorem 3.1 and Theorem 3.2.

S.3. Proof of Lemma 3.2. Under H_a , recall the definition of \mathcal{U} cited here as

$$(S.1) \quad \mathcal{U} = \left(\mu_1, \mu_{k_1+1}, \mu_{k_2+1}, \dots, \mu_{k_s+1} \right)$$

to be the matrix of distinct mean vectors. Let

$$(S.2) \quad \mathcal{V} = \left(\underbrace{a_{(1)}, \dots, a_{(1)}}_{k_1}, \underbrace{a_{(2)}, \dots, a_{(2)}}_{k_2-k_1}, \dots, \underbrace{a_{(s+1)}, \dots, a_{(s+1)}}_{n-k_s} \right),$$

where $a_{(i)}$ is the $(s+1) \times 1$ vector whose i th element is 1 and the others are 0.

With the definition, we can write the observation matrix $X = (X_1, X_2, \dots, X_n)$ as

$$X = \mathcal{U}\mathcal{V} + \Sigma_p^{1/2} Z,$$

where $Z = (Z_1, Z_2, \dots, Z_n)$. Further, call $P_0 = I_n - n^{-1} \mathbf{1}_n \mathbf{1}_n^T$. The pooled sample covariance matrix is then

$$\begin{aligned} S_n &= \frac{1}{n} \sum_{j=1}^n (X_j - \bar{X})(X_j - \bar{X})^T = \frac{1}{n} X P_0 X^T \\ &= \frac{1}{n} \Sigma_p^{1/2} Z P_0 Z^T \Sigma_p^{1/2} + \frac{1}{n} \Sigma_p^{1/2} Z P_0 \mathcal{V}^T \mathcal{U}^T \\ &\quad + \frac{1}{n} \mathcal{U} \mathcal{V} P_0 Z^T \Sigma_p^{1/2} + \frac{1}{n} \mathcal{U} \mathcal{V} \mathcal{V}^T \mathcal{U}^T \\ &= \tilde{S}_n + \frac{1}{n} \Sigma_p^{1/2} Z P_0 \mathcal{V}^T \mathcal{U}^T + \frac{1}{n} \mathcal{U} \mathcal{V} P_0 Z^T \Sigma_p^{1/2} + \frac{1}{n} \mathcal{U} \mathcal{V} \mathcal{V}^T \mathcal{U}^T \end{aligned}$$

It is straightforward that $A := S_n - \tilde{S}_n$ is of rank at most $3(s+1)$.

Recall that F_p is the spectral distribution of S_n . Denote the spectral distribution of \tilde{S}_n to be \tilde{F}_p . Using Lemma S.1.1, we obtain a deterministic bound on the distance between F_p and \tilde{F}_p as

$$\|F_p - \tilde{F}_p\|_\infty \leq \frac{1}{p} \text{rank}(A) \leq \frac{3(s+1)}{p} \rightarrow 0, \quad \text{as } p \rightarrow \infty.$$

For any $\lambda > 0$, consider

$$m_n(-\lambda) - \tilde{m}_n(-\lambda) = \int \frac{1}{\tau + \lambda} dF_p(x) - \int \frac{1}{\tau + \lambda} d\tilde{F}_p(\tau) = \int \frac{1}{\tau + \lambda} d\Delta(\tau),$$

where $\Delta(\tau) = F_p(\tau) - \tilde{F}_p(\tau)$. Note that both S_n and \tilde{S}_n are positive semi-definite. Therefore, $\Delta(\tau) = 0$ for any $\tau < 0$ and $\Delta(\infty) = \lim_{\tau \rightarrow \infty} \Delta(\tau) = 0$. By integration by parts,

$$|m_n(-\lambda) - \tilde{m}_n(-\lambda)| = \left| \int_0^\infty \frac{\Delta(\tau)}{(\tau + \lambda)^2} d\tau \right| \leq \|\Delta\|_\infty \int_0^\infty \frac{1}{(\tau + \lambda)^2} d\tau \leq \frac{3(s+1)}{p\lambda}.$$

Similar arguments lead to

$$|m'_n(-\lambda) - \tilde{m}'_n(-\lambda)| \leq \frac{3(s+1)}{p\lambda^2}.$$

The bound on the difference $\hat{\Theta}(\lambda) - \tilde{\Theta}(\lambda)$ and $\hat{\Gamma}(\lambda) - \tilde{\Gamma}(\lambda)$ follow easily from the fact that they are smooth functions of $m_n(-\lambda)$, $m'_n(-\lambda)$, $\tilde{m}_n(-\lambda)$, and $\tilde{m}'_n(-\lambda)$.

Lastly, consider the difference between

$$\begin{aligned} & \left| p^{-1} \text{tr}[(S_n + \lambda I_p)^{-1} A] - p^{-1} \text{tr}[(\tilde{S}_n + \lambda I_p)^{-1} A] \right| \\ &= p^{-1} \left| \text{tr} \left[\{(S_n + \lambda I_p)^{-1} - (\tilde{S}_n + \lambda I_p)^{-1}\} A \right] \right| \\ &\leq p^{-1} \left[\|(S_n + \lambda I_p)^{-1}\|_2 + \|(\tilde{S}_n + \lambda I_p)^{-1}\|_2 \right] \|A\|_2 \\ &\quad \times \text{rank} \left((S_n + \lambda I_p)^{-1} - (\tilde{S}_n + \lambda I_p)^{-1} \right) \\ &\leq p^{-1} \frac{2\|A\|_2}{\lambda} 3(s+1). \end{aligned}$$

It follows that the convergence results in Lemma 3.1 still hold under H_a .

S.4. Proof of Theorem 3.3 and Theorem 3.5. In this section, we prove Theorem 3.3 and Theorem 3.5. Clearly, the former is the special case of the latter when $s = 1$. Therefore, we directly work with Theorem 3.5.

First of all, it is straightforward that

$$\frac{1}{(1 + \sqrt{\gamma_n})^2 \ell_{\max}(\Sigma_p) + \lambda} \leq \ell_{\min}(\mathcal{D}_p(\lambda)) \leq \ell_{\max}(\mathcal{D}_p(\lambda)) \leq \frac{1}{\lambda}.$$

Under the assumed regime

$$\sqrt{p} \|\mathcal{U}^T \mathcal{D}_p(\lambda) \mathcal{U}\|_2 \asymp 1,$$

it is straightforward that $\sqrt{p} \|\mathcal{U}^T \mathcal{U}\|_2 \asymp 1$. It implies that the mean vectors are such that

$$\sup_j \sqrt{p} \|\mu_j\|_2^2 \asymp 1.$$

Secondly, recall the definition of $\tilde{u}_n(t_1, t_2, t_3)$ in (S.5) and the definition of \mathcal{V} in (S.2). We have

$$\begin{aligned} \frac{1}{\sqrt{n}} \mathcal{V} \tilde{u}_n(t_1, t_2, t_3) &= \left[\int u(x; t_1, t_2, t_3) v_j(x) dx \right]_{j=1}^{s+1} + O\left(\frac{1}{n}\right) \\ &= \sqrt{\kappa(t_1, t_2, t_3)} \psi(t_1, t_2, t_3) + O\left(\frac{1}{n}\right). \end{aligned}$$

The convergence is uniform in $(t_1, t_2, t_3) \in \mathcal{T}(\varepsilon)$. Moreover,

$$\frac{N(t_1, t_2, t_3)}{n} = \left(\kappa(t_1, t_2, t_3) \right)^{-1} + O(n^{-1}) = \left(\frac{1}{t_2 - t_1} + \frac{1}{t_3 - t_2} \right)^{-1} + O(n^{-1}).$$

Again, the convergence is uniform in $(t_1, t_2, t_3) \in \mathcal{T}(\varepsilon)$.

With these definitions

$$C_\lambda(t_1, t_2, t_3) = \frac{1}{\sqrt{n}} (S_n + \lambda I_p)^{-1/2} X \tilde{u}_n(t_1, t_2, t_3).$$

$$\begin{aligned} p^{-1} V_\lambda(t_1, t_2, t_3) &= \frac{N(t_1, t_2, t_3)}{p} \frac{1}{n} \left(\tilde{u}_n(t_1, t_2, t_3) \right)^T X^T (S_n + \lambda I_p)^{-1} X \tilde{u}_n(t_1, t_2, t_3) \\ &= \frac{N(t_1, t_2, t_3)}{p} \frac{1}{n} \left(\tilde{u}_n(t_1, t_2, t_3) \right)^T Z^T \Sigma_p^{1/2} (S_n + \lambda I_p)^{-1} \Sigma_p^{1/2} Z \tilde{u}_n(t_1, t_2, t_3) \\ &\quad + \frac{N(t_1, t_2, t_3)}{p} \left(\frac{1}{\sqrt{n}} \mathcal{V} \tilde{u}_n(t_1, t_2, t_3) \right)^T \mathcal{U}^T (S_n + \lambda I_p)^{-1} \mathcal{U} \left(\frac{1}{\sqrt{n}} \mathcal{V} \tilde{u}_n(t_1, t_2, t_3) \right) \\ &\quad + \frac{N(t_1, t_2, t_3)}{p\sqrt{n}} \left(\frac{1}{\sqrt{n}} \mathcal{V} \tilde{u}_n(t_1, t_2, t_3) \right)^T \mathcal{U}^T (S_n + \lambda I_p)^{-1} \Sigma_p^{1/2} Z \tilde{u}_n(t_1, t_2, t_3) \\ &\quad + \frac{N(t_1, t_2, t_3)}{p\sqrt{n}} \left(\tilde{u}_n(t_1, t_2, t_3) \right)^T Z^T \Sigma_p^{1/2} (S_n + \lambda I_p)^{-1} \mathcal{U} \left(\frac{1}{\sqrt{n}} \mathcal{V} \tilde{u}_n(t_1, t_2, t_3) \right) \\ &= A_1 + A_2 + A_3 + A_3^T, \quad \text{say.} \end{aligned}$$

We deal with A_1 , A_2 , and A_3 separately. Recall the definition of \tilde{S}_n as the pooled sample covariance matrix under the null hypothesis. Let

$$H = S_n - \tilde{S}_n = \frac{1}{n-1} \Sigma_p^{1/2} Z^T P_0 \mathcal{V}^T \mathcal{U}^T + \frac{1}{n-1} \mathcal{U} \mathcal{V} P_0 Z^T \Sigma_p^{1/2} + \frac{1}{n-1} \mathcal{U} \mathcal{V} \mathcal{V}^T \mathcal{U}^T.$$

Then, it is straightforward to show that

$$\mathbb{E} \|H\|_2^m = \|\mathcal{U}^T \mathcal{U}\|_2^m = O(p^{-m/2}), \quad m \geq 1.$$

We shall use the following identity.

$$\begin{aligned} (S_n + \lambda I_p)^{-1} &= (\tilde{S}_n + \lambda I_p)^{-1} - (\tilde{S}_n + \lambda I_p)^{-1} H (\tilde{S}_n + \lambda I_p)^{-1} \\ (S.1) \quad &\quad + (S_n + \lambda I_p)^{-1} H (\tilde{S}_n + \lambda I_p)^{-1} H (\tilde{S}_n + \lambda I_p)^{-1}. \end{aligned}$$

First, consider the term A_1 . We expand $(S_n + \lambda I_p)^{-1}$ using (S.1) to get

$$\begin{aligned}
\text{(S.2)} \quad & \frac{1}{n} \left(\tilde{u}_n(t_1, t_2, t_3) \right)^T Z^T \Sigma_p^{1/2} (S_n + \lambda I_p)^{-1} \Sigma_p^{1/2} Z \tilde{u}_n(t_1, t_2, t_3) \\
&= \frac{1}{n} \left(\tilde{u}_n(t_1, t_2, t_3) \right)^T Z^T \Sigma_p^{1/2} (\tilde{S}_n + \lambda I_p)^{-1} \Sigma_p^{1/2} Z \tilde{u}_n(t_1, t_2, t_3) \\
&\quad - \frac{1}{n} \left(\tilde{u}_n(t_1, t_2, t_3) \right)^T Z^T \Sigma_p^{1/2} (\tilde{S}_n + \lambda I_p)^{-1} H (\tilde{S}_n + \lambda I_p)^{-1} \Sigma_p^{1/2} Z \tilde{u}_n(t_1, t_2, t_3) \\
&\quad - \frac{1}{n} \left(\tilde{u}_n(t_1, t_2, t_3) \right)^T Z^T \Sigma_p^{1/2} (S_n + \lambda I_p)^{-1} H (\tilde{S}_n + \lambda I_p)^{-1} H (\tilde{S}_n + \lambda I_p)^{-1} \Sigma_p^{1/2} Z \tilde{u}_n(t_1, t_2, t_3).
\end{aligned}$$

The first term on the right-hand side of (S.2) is equivalent to the test statistic under the null hypothesis H_0 whose asymptotic distribution is shown to be $\{G(t_1, t_2, t_3)\}$ in Section S.2.

Next, we show that the second term is such that

$$\text{(S.3)} \quad \mathbb{E} \left| \frac{1}{n} \left(\tilde{u}_n(t_1, t_2, t_3) \right)^T Z^T \Sigma_p^{1/2} (\tilde{S}_n + \lambda I_p)^{-1} H (\tilde{S}_n + \lambda I_p)^{-1} \Sigma_p^{1/2} Z \tilde{u}_n(t_1, t_2, t_3) \right| \leq \mathcal{K} \frac{1}{\sqrt{p}} \|\mathcal{U}^T \mathcal{U}\|_2^{1/2}.$$

To this end, we first note that

$$\mathbb{E} \left\| \frac{1}{n(n-1)} \left(\tilde{u}_n(t_1, t_2, t_3) \right)^T Z^T \Sigma_p^{1/2} (\tilde{S}_n + \lambda I_p)^{-1} \Sigma_p^{1/2} Z^T P_0 \mathcal{V}^T \right\|_2^2 \leq \frac{\mathcal{K}}{n}.$$

which is due to arguments in Section S.2. In particular, for any regular vectors a, b ,

$$\mathbb{E} \left| \frac{1}{n} a^T Z^T \Sigma_p^{1/2} (\tilde{S}_n + \lambda I_p)^{-1} \Sigma_p^{1/2} Z b \right|^2 \leq \mathcal{K} \|a\|_2^2 \|b\|_2^2,$$

Secondly, we note that

$$\mathbb{E} \left\| \mathcal{U}^T (\tilde{S}_n + \lambda I_p)^{-1} \Sigma_p^{1/2} Z \tilde{u}_n(t_1, t_2, t_3) \right\|_2^2 \leq \mathcal{K} \|\mathcal{U}^T \mathcal{U}\|_2,$$

which is shown in Section S.4 of Li et al. (2020a) (See (S.4.4) therein). Thirdly, we have

$$\begin{aligned}
& \mathbb{E} \left| \frac{1}{n(n-1)} \left(\tilde{u}_n(t_1, t_2, t_3) \right)^T Z^T \Sigma_p^{1/2} (\tilde{S}_n + \lambda I_p)^{-1} \mathcal{U} \mathcal{V} \mathcal{V}^T \mathcal{U}^T \right. \\
& \quad \left. (\tilde{S}_n + \lambda I_p)^{-1} \Sigma_p^{1/2} Z \tilde{u}_n(t_1, t_2, t_3) \right| \\
& \leq \frac{\mathcal{K} \|\mathcal{U}^T \mathcal{U}\|_2}{n} \mathbb{E} \left(\tilde{u}_n(t_1, t_2, t_3) \right)^T Z^T Z \tilde{u}_n(t_1, t_2, t_3) = \mathcal{K} \|\mathcal{U}^T \mathcal{U}\|_2.
\end{aligned}$$

It completes the proof of (S.3).

As for the third term on the right-hand side of (S.2), a simple spectral norm bound indicates that

$$\begin{aligned}
& \mathbb{E} \left| \frac{1}{n} \left(\tilde{u}_n(t_1, t_2, t_3) \right)^T Z^T \Sigma_p^{1/2} (S_n + \lambda I_p)^{-1} H (\tilde{S}_n + \lambda I_p)^{-1} H (\tilde{S}_n + \lambda I_p)^{-1} \Sigma_p^{1/2} Z \tilde{u}_n(t_1, t_2, t_3) \right| \\
& \leq (\mathbb{E} \|H\|_2^4)^{1/2} \left(\mathbb{E} \left| \frac{1}{n} \left(\tilde{u}_n(t_1, t_2, t_3) \right)^T Z^T Z \tilde{u}_n(t_1, t_2, t_3) \right|^2 \right)^{1/2} \\
& \leq \mathcal{K} \frac{1}{\sqrt{p}} \|\mathcal{U}^T \mathcal{U}\|_2.
\end{aligned}$$

Together,

$$A_1 = \frac{N(t_1, t_2, t_3)}{p} \frac{1}{n} \left(\tilde{u}_n(t_1, t_2, t_3) \right)^T Z^T \Sigma_p^{1/2} (\tilde{S}_n + \lambda I_p)^{-1} \Sigma_p^{1/2} Z \tilde{u}_n(t_1, t_2, t_3) + o_p \left(\frac{1}{\sqrt{p}} \right).$$

Therefore,

$$\sqrt{p} \frac{A_1 - \hat{\Theta}(\lambda)}{\sqrt{\hat{\Gamma}(\lambda)}} \rightsquigarrow \{G(t_1, t_2, t_3), (t_1, t_2, t_3) \in \mathcal{T}(\varepsilon)\}.$$

To deal with A_2 , we aim to show the following results

$$(S.4) \quad \sqrt{p} \mathcal{U}^T (S_n + \lambda I_p)^{-1} \mathcal{U} = \sqrt{p} \mathcal{U}^T \mathcal{D}_p(\lambda) \mathcal{U} + o_p(1).$$

Using the well-established local laws of \tilde{S}_n in RMT (Theorem 3.6 of [Knowles and Yin \(2017\)](#)), we have

$$\sqrt{p} \mathcal{U}^T (\tilde{S}_n + \lambda I_p)^{-1} \mathcal{U} = \sqrt{p} \mathcal{U}^T \mathcal{D}_p(\lambda) \mathcal{U} + o_p(1).$$

Here, we are using the fact that $\sqrt{p} \|\mathcal{U}^T \mathcal{U}\|_2 \simeq 1$. It then suffices to bound the difference

$$\sqrt{p} \mathcal{U}^T (S_n + \lambda I_p)^{-1} \mathcal{U} - \sqrt{p} \mathcal{U}^T (\tilde{S}_n + \lambda I_p)^{-1} \mathcal{U}.$$

Again, using the identity (S.1),

$$\begin{aligned} & \sqrt{p} \mathbb{E} \left\| \mathcal{U}^T \left[(S_n + \lambda I_p)^{-1} - (\tilde{S}_n + \lambda I_p)^{-1} \right] \mathcal{U} \right\|_2 \\ &= \sqrt{p} \mathbb{E} \left\| \mathcal{U}^T (\tilde{S}_n + \lambda I_p)^{-1} H (\tilde{S}_n + \lambda I_p)^{-1} \mathcal{U} \right\|_2 \\ & \quad + \sqrt{p} \mathbb{E} \left\| \mathcal{U}^T (S_n + \lambda I_p)^{-1} H (\tilde{S}_n + \lambda I_p)^{-1} H (\tilde{S}_n + \lambda I_p)^{-1} \mathcal{U} \right\|_2 \\ &\leq \mathcal{K} \sqrt{p} \mathbb{E} \|H\|_2 \|\mathcal{U}^T \mathcal{U}\|_2 + \mathcal{K} \sqrt{p} \mathbb{E} \|H\|_2^2 \|\mathcal{U}^T \mathcal{U}\| \\ &= \mathcal{K} \|\mathcal{U}^T \mathcal{U}\|. \end{aligned}$$

Therefore, we conclude that

$$\sqrt{p} \mathcal{U}^T \left[(\tilde{S}_n + \lambda I_p)^{-1} - (S_n + \lambda I_p)^{-1} \right] \mathcal{U} = o_p(1).$$

Together, (S.4) is proved.

Combined with the convergence of $N(t_1, t_2, t_3)/n$ and $\frac{1}{\sqrt{n}} \mathcal{V} \tilde{u}_n(t_1, t_2, t_3)$, we claim that

$$\begin{aligned} \sqrt{p} A_2 &= \frac{1}{\gamma_n} \left(\psi(t_1, t_2, t_3) \right)^T \mathcal{U}^T \mathcal{D}_p(\lambda) \mathcal{U} \psi(t_1, t_2, t_3) + o_p(1) \\ &= \frac{1}{\gamma_n} Q_p(t_1, t_2, t_3; \lambda, \mathcal{U}) + o_p(1). \end{aligned}$$

Here, the residual $o_p(1)$ above indicates a matrix whose spectral norm is $o_p(1)$, uniformly in $(t_1, t_2, t_3) \in \mathcal{T}(\varepsilon)$.

The treatment of A_3 is similar to the arguments for A_1 and we show that

$$\sqrt{p} \|A_3\|_2 = o_p(1).$$

We omit the details.

Combining the analysis of A_1, A_2, A_3 , we conclude that under the assumed local alternatives, uniformly for $(t_1, t_2, t_3) \in \mathcal{T}(\varepsilon)$,

$$\sqrt{p} \frac{p^{-1} V_\lambda(t_1, t_2, t_3) - \hat{\Theta}(\lambda)}{\sqrt{\hat{\Gamma}(\lambda)}}$$

$$= \sqrt{p} \frac{p^{-1} V_\lambda^{(0)}(t_1, t_2, t_3) - \hat{\Theta}(\lambda)}{\sqrt{\hat{\Gamma}(\lambda)}} + \frac{Q_p(t_1, t_2, t_3; \lambda, \mathcal{U})}{\gamma_n \Gamma_n^{1/2}} + o_p(1).$$

The form of the power function stated in Theorem 3.3 follows.

S.5. Proof of Theorem 3.4 and Theorem 3.6. In this section, we prove Theorem 3.4 and Theorem 3.6. Since the former is the special case of the latter when $s = 1$, we directly work under the setup of Theorem 3.6. Throughout the section, $\mathbb{P}_\mathcal{U}$ is the prior probability measure of \mathcal{U} under **PA-MC**, and $\mathbb{P}(\cdot | \mathcal{U})$ is the probability measure of the observations conditional on \mathcal{U} , and \mathbb{P}_Z is the probability measure of Z .

Under **PA-MC**, using the concentration inequality as in Lemma S.1.4, we can show that

$$\left\| \sqrt{p} \mathcal{U}^T \mathcal{U} - p^{-1} \text{tr}(B) \Omega \Omega^T \right\|_2 \xrightarrow{\mathbb{P}_\mathcal{U}} 0.$$

and also for any fixed $\lambda > 0$,

$$(S.1) \quad \left\| \sqrt{p} \mathcal{U}^T \mathcal{D}_p(\lambda) \mathcal{U} - q_p(\lambda, B) \Omega \Omega^T \right\|_2 \xrightarrow{\mathbb{P}_\mathcal{U}} 0.$$

Since $\|B\|_2$ is bounded and Ω is fixed, for any $\zeta > 0$, there exists a sufficiently large constant \mathcal{K}_ζ and N_1 such that when $n > N_1$,

$$\mathbb{P}_\mathcal{U} \left(K^{(1)}(\zeta) \right) > 1 - \zeta/4,$$

where

$$K^{(1)}(\zeta) = \left\{ \mathcal{U} : \left\| \sqrt{p} \mathcal{U}^T \mathcal{U} \right\|_2 \leq \mathcal{K}_\zeta \right\}.$$

Moreover, for any $\varphi > 0$ and $\zeta > 0$, there exists a sufficiently large N_2 such that when $n > N_2$,

$$\mathbb{P}_\mathcal{U} \left(K^{(2)}(\zeta, \varphi) \right) > 1 - \zeta/4,$$

where

$$K^{(2)}(\zeta, \varphi) = \left\{ \mathcal{U} : \sup_{\mathcal{T}(\varepsilon)} \frac{1}{\gamma_n \Gamma_n(\lambda)} \left| \tilde{u}_n^T(t_1, t_2, t_3) \left(\sqrt{p} \mathcal{U}^T \mathcal{D}_p(\lambda) \mathcal{U} - q_p(\lambda, B) \Omega \Omega^T \right) \tilde{u}_n(t_1, t_2, t_3) \right| \leq \varphi/4 \right\}.$$

It implies that when $n > \max(N_1, N_2)$,

$$(S.2) \quad \mathbb{P}_\mathcal{U} \left(K^{(1)}(\zeta) \cap K^{(2)}(\zeta, \varphi) \right) \geq 1 - \zeta/2.$$

For convenience, define

$$\beta_p^*(\xi_{\text{mc}}(1 - \alpha, \varepsilon)) = \mathbb{P} \left(\sup_{\mathcal{T}(\varepsilon)} \left\{ G(t_1, t_2, t_3) + \frac{q_p(\lambda, B)}{\gamma_n \Gamma_n^{1/2}(\lambda)} \left\| \Omega^T \psi(t_1, t_2, t_3) \right\|_2^2 \right\} > \xi_{\text{mc}}(1 - \alpha, \varepsilon) \right).$$

Therefore, to show the convergence in probability of

$$\beta_{\text{mc}}(\lambda, \mathcal{U}) - \beta_p^*(\xi_{\text{mc}}(1 - \alpha, \varepsilon))$$

with respect to $\mathbb{P}_\mathcal{U}$, it suffices to assume that $\mathcal{U} \in K^{(1)}(\zeta) \cap K^{(2)}(\zeta, \varphi)$. Namely, we only need to show that for any fixed $\varphi > 0$ and $\zeta > 0$, we can find a sufficiently large constant N_0 such that when $n > N_0$,

$$(S.3) \quad \mathbb{P}_\mathcal{U} \left(\left\{ \left| \beta_{\text{mc}}(\lambda, \mathcal{U}) - \beta_p^*(\xi_{\text{mc}}(1 - \alpha, \varepsilon)) \right| > 2\varphi \right\} \cap \left\{ K^{(1)}(\zeta) \cap K^{(2)}(\zeta, \varphi) \right\} \right) < \zeta/2.$$

It is because that, combining (S.2) and (S.3), when $n > \max(N_1, N_2, N_0)$, we have

$$\begin{aligned} \mathbb{P}_{\mathcal{U}}\left(|\beta_{\text{mc}}(\lambda, \mathcal{U}) - \beta_p^*| > 2\varphi\right) &\leq \mathbb{P}_{\mathcal{U}}\left(\left\{|\beta_{\text{mc}}(\lambda, \mathcal{U}) - \beta_p^*| > 2\varphi\right\} \cap \left\{K^{(1)}(\zeta) \cap K^{(2)}(\zeta, \varphi)\right\}\right) \\ &+ \mathbb{P}_{\mathcal{U}}\left(\left\{K^{(1)}(\zeta) \cap K^{(2)}(\zeta, \varphi)\right\}^C\right) \leq \zeta. \end{aligned}$$

Therefore, in the following analysis, without further mentioning, we assume that $\mathcal{U} \in K^{(1)}(\zeta) \cap K^{(2)}(\zeta, \varphi)$.

For convenience, denote

$$\begin{aligned} \tilde{D}_{\lambda}(t_1, t_2, t_3) &= \sqrt{p} \frac{\frac{N(t_1, t_2, t_3)}{p} \frac{1}{n} \left(\tilde{u}_n(t_1, t_2, t_3)\right)^T Z^T \Sigma_p^{1/2} (\tilde{S}_n + \lambda I_p)^{-1} \Sigma_p^{1/2} Z \tilde{u}_n(t_1, t_2, t_3)}{\Gamma_n^{1/2}(\lambda)} \\ &+ \frac{1}{\gamma_n \Gamma_n^{1/2}(\lambda)} q_p(\lambda, B) \|\Omega^T \psi(t_1, t_2, t_3)\|_2^2 \end{aligned}$$

In Section S.4, we showed that conditional on \mathcal{U} , the standardized statistic

$$\sqrt{p} \frac{p^{-1} V_{\lambda}(t_1, t_2, t_3) - \Theta_n(\lambda)}{\Gamma_n^{1/2}(\lambda)},$$

is such that

$$\sup_{\mathcal{T}(\varepsilon)} \left| \sqrt{p} \frac{p^{-1} V_{\lambda}(t_1, t_2, t_3) - \Theta_n(\lambda)}{\Gamma_n^{1/2}(\lambda)} - \tilde{D}_{\lambda}(t_1, t_2, t_3) \right| \xrightarrow{\mathbb{P}(\cdot|\mathcal{U})} 0$$

with a tail bound only depends on $\|\mathcal{U}^T \mathcal{U}\|_2$. Moreover, Lemma 3.1 and Lemma 3.2 indicate that with a tail bound independent of \mathcal{U} , we have

$$\hat{\Theta}(\lambda) - \Theta_n(\lambda) \xrightarrow{\mathbb{P}(\cdot|\mathcal{U})} 0, \quad \hat{\Gamma}(\lambda) - \Gamma_n(\lambda) \xrightarrow{\mathbb{P}(\cdot|\mathcal{U})} 0.$$

Combining the results, we conclude that for any $\varphi > 0$ and $\zeta > 0$, we can find a sufficiently large N_3 such that when $n > N_3$,

$$\mathbb{P}\left(K^{(3)} \mid \mathcal{U} \in K^{(1)}(\zeta) \cap K^{(2)}(\zeta, \varphi)\right) > 1 - \varphi/2,$$

where

$$K^{(3)} = \left\{ (Z, \mathcal{U}) : \sup_{\mathcal{T}(\varepsilon)} |D_{\lambda}(t_1, t_2, t_3) - \tilde{D}_{\lambda}(t_1, t_2, t_3)| < \varphi/2 \right\}$$

It indicates that we can approximate the distribution function of $D_{\lambda}(t_1, t_2, t_3)$ giving \mathcal{U} using that of $\tilde{D}_{\lambda}(t_1, t_2, t_3)$.

Since

$$\begin{aligned} \beta_{\text{mc}}(\lambda, \mathcal{U}) &= \mathbb{P}\left(\sup_{\mathcal{T}(\varepsilon)} D_{\lambda}(t_1, t_2, t_3) > \xi_{\text{mc}}(1 - \alpha, \varepsilon) \mid \mathcal{U}\right) \\ &= \mathbb{P}\left(\left\{\sup_{\mathcal{T}(\varepsilon)} D_{\lambda}(t_1, t_2, t_3) > \xi_{\text{mc}}(1 - \alpha, \varepsilon)\right\} \cap K^{(3)} \mid \mathcal{U}\right) \\ &+ \mathbb{P}\left(\left\{\sup_{\mathcal{T}(\varepsilon)} D_{\lambda}(t_1, t_2, t_3) > \xi_{\text{mc}}(1 - \alpha, \varepsilon)\right\} \cap \{K^{(3)}\}^c \mid \mathcal{U}\right), \end{aligned}$$

it follows that when $n > \max(N_1, N_2, N_3)$ and $\mathcal{U} \in K^{(1)}(\zeta) \cap K^{(2)}(\zeta, \varphi)$,

$$\beta_{\text{mc}}(\lambda, \mathcal{U}) \leq \varphi/2 + \mathbb{P}_Z \left(\sup_{\mathcal{T}(\varepsilon)} \tilde{D}_\lambda(t_1, t_2, t_3) > \xi_{\text{mc}}(1 - \alpha, \varepsilon) - \varphi/2 \right),$$

$$\beta_{\text{mc}}(\lambda, \mathcal{U}) \geq -\varphi/2 + \mathbb{P}_Z \left(\sup_{\mathcal{T}(\varepsilon)} \tilde{D}_\lambda(t_1, t_2, t_3) > \xi_{\text{mc}}(1 - \alpha, \varepsilon) + \varphi/2 \right).$$

Using the arguments in Section S.2, we immediately obtain that there exists a constant N_4 such that when $n > N_4$

$$\left| \mathbb{P}_Z \left(\tilde{D}_\lambda(t_1, t_2, t_3) > \xi_{\text{mc}}(1 - \alpha, \varepsilon) - \varphi/2 \right) - \beta_p^*(\xi_{\text{mc}}(1 - \alpha, \varepsilon) - \varphi/2) \right| < \varphi/2,$$

$$\left| \mathbb{P}_Z \left(\tilde{D}_\lambda(t_1, t_2, t_3) > \xi_{\text{mc}}(1 - \alpha, \varepsilon) + \varphi/2 \right) - \beta_p^*(\xi_{\text{mc}}(1 - \alpha, \varepsilon) + \varphi/2) \right| < \varphi/2,$$

It follows then, when $n > \max(N_1, N_2, N_3, N_4)$ and $\mathcal{U} \in K^{(1)}(\zeta) \cap K^{(2)}(\zeta, \varphi)$,

$$\beta_{\text{mc}}(\lambda, \mathcal{U}) \leq \varphi + \beta_p^*(\xi_{\text{mc}}(1 - \alpha, \varepsilon) - \varphi/2),$$

$$\beta_{\text{mc}}(\lambda, \mathcal{U}) \geq -\varphi + \beta_p^*(\xi_{\text{mc}}(1 - \alpha, \varepsilon) + \varphi/2).$$

It implies that (S.3) holds when φ is sufficiently small. It completes the proof.

S.6. Proof of Lemma 4.1. Recall that $\varphi_n(z)$ is the Stieltjes transform of a probability measure determined through the M-P equation. We denote the measure as F_n in the subsequent analysis. That is,

$$\varphi_n(z) = \int \frac{dF_n(\tau)}{\tau - z}.$$

Define $s_n(z)$

$$s_n(z) = \frac{1 - \gamma_n}{-z} + \gamma_n \varphi_n(z).$$

Then, it is straightforward to verify that $s_n(z)$ is the Stieltjes transform of a probability measure \tilde{F}_n . The two distributions differ only on a point mass at $\tau = 0$. Indeed, if $\gamma_n \leq 1$,

$$d\tilde{F}_n(\tau) = \gamma_n dF_n(\tau) + (1 - \gamma_n) \mathbb{1}_0(\tau).$$

Conversely, if $\gamma_n > 1$,

$$dF_n(\tau) = \frac{1}{\gamma_n} d\tilde{F}_n(\tau) + (1 - 1/\gamma_n) \mathbb{1}_0(\tau).$$

We can write

$$s_n(z) = \int \frac{d\tilde{F}_n(\tau)}{\tau - z}.$$

With the definition, we can write

$$\begin{aligned} \Gamma_n(\lambda) &= (1 - \gamma_n + \gamma_n \lambda \varphi_n(-\lambda))(1 - \lambda \varphi_n(-\lambda)) - \lambda \varphi_n(-\lambda) + \lambda^2 \varphi_n'(-\lambda) \\ &= \lambda s_n(-\lambda) \frac{1 - \lambda s_n(-\lambda)}{\gamma_n} + \frac{1 - \lambda s_n(-\lambda)}{\gamma_n} - 1 - \frac{1}{\gamma_n} (1 - \gamma_n - \lambda^2 s_n'(-\lambda)) \\ &= \frac{\lambda^2}{\gamma_n} [s_n'(-\lambda) - s_n^2(-\lambda)]. \end{aligned}$$

Call

$$f_0(\lambda) = \frac{\varphi_n(-\lambda)}{\sqrt{\Gamma_n(\lambda)}} = \frac{1}{\sqrt{\gamma_n}} \frac{s_n(-\lambda) - (1 - \gamma_n)/\lambda}{\lambda\sqrt{s'_n(-\lambda) - s_n^2(-\lambda)}}$$

$$f_1(\lambda) = \frac{1 - \lambda\varphi_n(-\lambda)}{\sqrt{\Gamma_n(\lambda)}} = \frac{1}{\sqrt{\gamma_n}} \frac{1 - \lambda s_n(-\lambda)}{\lambda\sqrt{s'_n(-\lambda) - s_n^2(-\lambda)}}.$$

We show that both $f_0(\lambda)$ and $f_1(\lambda)$ are monotonically decreasing function of λ .

For convenience, denote $U = U(X) = \lambda/(X + \lambda)$. Consider the first three moments of U when $X \sim \tilde{F}_n$ and when $X \sim F_n$ as

$$\alpha_j = \mathbb{E}_{F_n} U^j, \quad j = 1, 2, 3; \quad \beta_j = \mathbb{E}_{\tilde{F}_n} U^j, \quad j = 1, 2, 3.$$

The following relationship holds:

$$\begin{aligned} \gamma_n \alpha_1 + (1 - \gamma_n) &= \beta_1 = \lambda s_n(-\lambda), \\ \gamma_n \alpha_2 + (1 - \gamma_n) &= \beta_2 = \lambda^2 s'_n(-\lambda), \\ \gamma_n \alpha_3 + (1 - \gamma_n) &= \beta_3 = \frac{1}{2} \lambda^3 s''_n(-\lambda). \end{aligned}$$

With the notation,

$$\begin{aligned} \Gamma_n(\lambda) &= \frac{1}{\gamma_n} (\beta_2 - \beta_1^2), \\ \Gamma'_n(\lambda) &= \frac{1}{\gamma_n} \left(2\lambda s'_n(-\lambda) - 2\lambda s_n^2(-\lambda) + \lambda^2 (-s''_n(-\lambda) + 2s_n(-\lambda)s'_n(-\lambda)) \right) \\ &= \frac{2}{\gamma_n \lambda} (\beta_2 - \beta_1^2 - \beta_3 + \beta_1 \beta_2), \\ \varphi'_n(-\lambda) &= \frac{1}{\gamma_n} \left(s'_n(-\lambda) - \frac{1 - \gamma_n}{\lambda^2} \right) = \frac{1}{\lambda^2 \gamma_n} (\beta_2 - (1 - \gamma_n)). \end{aligned}$$

First, consider $f'_0(\lambda)$

$$\begin{aligned} f'_0(\lambda) &= \frac{-\varphi'_n(-\lambda)\sqrt{\Gamma_n(\lambda)} - \varphi_n(-\lambda)\frac{1}{2\sqrt{\Gamma_n(\lambda)}}\Gamma'_n(\lambda)}{\Gamma_n(\lambda)} \\ &= \frac{-\gamma_n \lambda^2 \varphi'_n(-\lambda)\Gamma_n(\lambda) - (\gamma_n/2)\lambda^2 \varphi_n(-\lambda)\Gamma'_n(\lambda)}{\gamma_n \lambda^2 (\Gamma_n(\lambda))^{3/2}} \\ &= \frac{(\beta_2 - (1 - \gamma_n))(\beta_2 - \beta_1^2) + (\beta_1 - (1 - \gamma_n))(\beta_2 - \beta_1^2 - \beta_3 + \beta_1 \beta_2)}{-\gamma_n \lambda^2 (\Gamma_n(\lambda))^{3/2}} \end{aligned}$$

It suffices to show the sign of the numerator is nonnegative.

$$\begin{aligned} &(\beta_2 - (1 - \gamma_n))(\beta_2 - \beta_1^2) + (\beta_1 - (1 - \gamma_n))(\beta_2 - \beta_1^2 - \beta_3 + \beta_1 \beta_2) \\ &= (\gamma_n - 1)(-2\beta_1^2 + \beta_1 \beta_2 + 2\beta_2 - \beta_3) + (\beta_2^2 - \beta_1 \beta_3 + \beta_1 \beta_2 - \beta_1^3) \end{aligned}$$

Take the first term on the right-hand side

$$-2\beta_1^2 + \beta_1 \beta_2 + 2\beta_2 - \beta_3 = \mathbb{E}_{\tilde{F}_n} (1 - U)(U - \beta_1)^2 + (1 - \beta_1)(\beta_2 - \beta_1^2).$$

Since $U(X) = \lambda/(X + \lambda) \leq 1$ with probability 1 when $X \sim \tilde{F}_n$, we have

$$-2\beta_1^2 + \beta_1\beta_2 + 2\beta_2 - \beta_3 \geq 0.$$

Take the second term on the right-hand side

$$\begin{aligned} \beta_2^2 - \beta_1\beta_3 + \beta_1\beta_2 - \beta_1^3 &= (\beta_2 - \beta_1^2)^2 + \beta_1(1 - \beta_1)(\beta_2 - \beta_1^2) - \beta_1\mathbb{E}_{\tilde{F}_n}(U - \beta_1)^3 \\ &= (\beta_2 - \beta_1^2)^2 + \beta_1\mathbb{E}_{\tilde{F}_n}\left((1 - \beta_1)(U - \beta_1)^2 - (U - \beta_1)^3\right) \\ &= (\beta_2 - \beta_1^2)^2 + \beta_1\mathbb{E}_{\tilde{F}_n}(U - \beta_1)^2(1 - U) \geq 0. \end{aligned}$$

If $\gamma_n \geq 1$, we immediately have $f'_0(\lambda) \geq 0$. It remains to show the same result when $\gamma_n < 1$. To this end, we re-express the term using α_1 , α_2 and α_3 .

$$\begin{aligned} &(\beta_2 - (1 - \gamma_n))(\beta_2 - \beta_1^2) + (\beta_1 - (1 - \gamma_n))(\beta_2 - \beta_1^2 - \beta_3 + \beta_1\beta_2) \\ &= \gamma_n^2 \left[(1 - \gamma_n)(1 - \alpha_1)(\alpha_2 - \alpha_1^2) + (\alpha_2^2 - \alpha_1\alpha_3 + \alpha_1\alpha_2 - \alpha_1^3) \right] \end{aligned}$$

Since $U(X) = \lambda/(X + \lambda) \leq 1$ when $X \sim F_n$,

$$\begin{aligned} \alpha_2^2 - \alpha_1\alpha_3 + \alpha_1\alpha_2 - \alpha_1^3 &= (\alpha_2 - \alpha_1^2)^2 + \alpha_1(1 - \alpha_1)(\alpha_2 - \alpha_1^2) - \alpha_1\mathbb{E}_{F_n}(U - \alpha_1)^3 \\ &= (\alpha_2 - \alpha_1^2)^2 + \alpha_1\mathbb{E}_{F_n}\left((1 - \alpha_1)(U - \alpha_1)^2 - (U - \alpha_1)^3\right) \\ &= (\alpha_2 - \alpha_1^2)^2 + \alpha_1\mathbb{E}_{F_n}(U - \alpha_1)^2(1 - U) \geq 0. \end{aligned}$$

We conclude that if $\gamma_n < 1$

$$\gamma_n^2 \left[(1 - \gamma_n)(1 - \alpha_1)(\alpha_2 - \alpha_1^2) + (\alpha_2^2 - \alpha_1\alpha_3 + \alpha_1\alpha_2 - \alpha_1^3) \right] \geq 0.$$

All together, we have $f'_0(\lambda) \leq 0$ on $\lambda \in (0, \infty)$.

Secondly, we consider $f_1(\lambda)$.

$$\begin{aligned} f'_1(\lambda) &= \frac{(\lambda s'_n(-\lambda) - s_n(-\lambda))\Gamma_n(\lambda) - (\lambda s_n(-\lambda) - \lambda^2 s_n^2(-\lambda))\frac{1}{2}\Gamma'_n(\lambda)}{\gamma_n(\lambda s_n(-\lambda))^2(\Gamma_n(\lambda))^{3/2}} \\ &= \frac{(\beta_1 - \beta_2)(\beta_2 - \beta_1^2) + \beta_1(1 - \beta_1)(\beta_2 - \beta_1^2 - \beta_3 + \beta_1\beta_2)}{-\gamma_n^2\lambda(\lambda s_n(-\lambda))^2(\Gamma_n(\lambda))^{3/2}} \end{aligned}$$

Again, it suffices to show the sign of the numerator is nonnegative.

$$\begin{aligned} &(\beta_1 - \beta_2)(\beta_2 - \beta_1^2) + (\beta_1 - \beta_1^2)(\beta_2 - \beta_3 - \beta_1^2 + \beta_1\beta_2) \\ &= \beta_1[(1 - \beta_1)(\beta_2 - \beta_3) - (\beta_1 - \beta_2)^2] + (1 - \beta_1)(\beta_1 - \beta_2)[\beta_2 - \beta_1^2] \end{aligned}$$

The first term on the right-hand side is such that

$$\begin{aligned} \beta_1 \det \left| \mathbb{E}_{\tilde{F}_n}(1 - U) \begin{pmatrix} 1 \\ U \end{pmatrix} (1 \ U) \right| &= \beta_1 \det \left| \mathbb{E}_{\tilde{F}_n} \begin{pmatrix} 1 - U & U(1 - U) \\ U(1 - U) & U^2(1 - U) \end{pmatrix} \right| \\ &= \beta_1 \det \left| \begin{pmatrix} 1 - \beta_1 & \beta_1 - \beta_2 \\ \beta_1 - \beta_2 & \beta_2 - \beta_3 \end{pmatrix} \right| = \beta_1(1 - \beta_1)(\beta_2 - \beta_3) - \beta_1(\beta_1 - \beta_2)^2 \end{aligned}$$

While $(1 - U) \geq 0$, the matrix

$$(1 - U) \begin{pmatrix} 1 \\ U \end{pmatrix} (1 \ U)$$

is nonnegative definite with probability 1. Therefore, its mean is also nonnegative definite. Therefore, $\beta_1(1 - \beta_1)(\beta_2 - \beta_3) - \beta_1(\beta_1 - \beta_2)^2 \geq 0$.

The second term on the right-hand side is such that

$$1 - \beta_1 \geq 0, \quad \beta_1 - \beta_2 = \mathbb{E}_{\tilde{F}_n} U(1 - U) \geq 0, \quad \text{and } \beta_2 - \beta_1^2 = \text{Var}_{\tilde{F}_n}(U) \geq 0.$$

All together, we conclude that $f'_1(\lambda) \leq 0$.